

## **ABSTRACT**

DUVAL, LUIS DENIT. Low Power Valve Actuation using Trans-Permanent Magnetics.

(Under the Direction of Dr. Lawrence M. Silverberg.)

The subject of magnetic actuators is very broad, and encompasses a wide range of technologies, magnetic circuit topologies, and performance characteristics for an ever-increasing spectrum of applications. As a consequence of recent advances in soft and hard magnetic materials and developments in power electronics, microprocessors and digital control strategies, and the continuing demand for higher performance motion control systems, there appears to be more research and development activity in magnetic actuators for applications spanning all market sectors than at any time. Thus many actuator types and topologies are emerging with widely varying operational characteristics, in terms of displacement (rotary or linear), speed of response, position accuracy and duty cycle.

In this dissertation, a rational approach for switching the states of permanent magnets through an on-board magnetization process is presented. The resulting dynamic systems are referred to as trans-permanent magnetic systems (*T-PM*). The first part of this research focuses on the governing equations needed for the analysis of trans-permanent magnetic systems. Their feasibility is demonstrated experimentally. In doing so, a method that has the potential of leading to new ultra-low power designs for electromechanical devices is introduced.

In the second part of this research, the aforementioned developments in *T-PM* are applied to the problem of low power valves. Whereas alternate approaches to low power valve control may utilize latching to maintain valve position during inactive periods, an approach that eliminates the need for latching mechanisms is presented. Instead, the principles of *T-PM* are employed to switch the states of permanent magnets; the use of permanent magnets instead of electromagnets eliminates power consumption during inactive periods, thereby reducing power consumption to ultra-low levels.

The magnets in a *T-PM* actuator are configured in a stack. The relationships between the strength and number of magnets in the stack and the stroke and resolution of the actuator are developed. This dissertation reports on the design and testing of a prototype valve actuator that uses a stack of *T-PM* with alternating polarity. It is shown that this stack is well suited for discrete state process valves having a small number of states. It is concluded that the trans-permanent valve represents a promising valve actuation technology.

# **LOW POWER VALVE ACTUATION USING TRANS-PERMANENT MAGNETICS**

by

**Luis D. Duval**

A dissertation submitted to the Graduate Faculty of  
North Carolina State University  
in partial fulfillment of the requirements for the Degree of  
Doctor of Philosophy

**DEPARTMENT OF MECHANICAL AND AEROSPACE ENGINEERING**

Raleigh

2003

**APPROVED BY:**

---

Dr. Lawrence M. Silverberg  
Chairman of Advisory Committee

---

Dr. Gregory D. Buckner

---

Dr. Richard F. Keltie

---

Dr. Mohammed A. Zikry

*A la memoria imperecedera de mi padre,  
guia imperdurable de mis pasos.  
A todos los que creyeron y confiaron en mi.*

## **BIOGRAPHY**

Luis D. Duval was born the in Province El Oro, Ecuador. He attended the Technical University of Machala where he got his B.S in Civil Engineering in 1986. After completing his undergraduate studies, Luis pursued advanced studies in Structural Engineering in the Institute for Research and Advanced Studies at the State University of Guayaquil, Ecuador where he got a specialization on the field in early 1988. From 1988 to 1991 he taught in the Department of Civil Engineering at Technical University of Machala, Ecuador. In 1995 the author was admitted to the Department of Mechanical Engineering at Worcester Polytechnic Institute in Worcester, Massachusetts. During his two years of study towards to his M.S. degree he worked in the field of probabilistic mechanics. In January 2000 he transferred to the graduate program in the Department of Mechanical and Aerospace Engineering at North Carolina State University in Raleigh, North Carolina. During his studies he worked as a research assistant, taught undergraduate courses and worked as an engineer specialist in research and development field. He married “the most beautiful girl” from Ecuador, Maria Esther Ruilova and he has two boys, Jhostyn and Steven. The author is currently working as Engineering Specialist at Thomas Lord Research Center, Lord Corporation; Cary, North Carolina in the Mechanical Research and Development Division.

## ACKNOWLEDGMENTS

The author would like to express his deepest gratitude to Dr. Larry M. Silverberg. Throughout this research, he supervised my progress, helped me, had patience, advised me and his friendship in every phase of this study are appreciated. I have always believed that an advisor has to be loyal and friend to his students and he has been all. I truly treasure the opportunity of being associated with him. “Doc”, thank you very much for giving me the opportunity to be both your friend and student.

I would like to thank my dissertation committee members; Dr. Gregory D. Buckner, Dr. Richard F. Keltie, and Dr. Mohammed. A. Zikry. My gratitude also goes to Mr. Michael BreedLove and Mr. Rufus Richardson for all their patience showed during the last months meanwhile I was designing and testing my valve prototype.

The author conveys his gratitude and respect for all his teachers in Ecuador, who were a source of inspiration, strength, and love for science; especially, Professor Luis Cobo-Saénz and Professor José Palacio-González, from the Technical University of Machala and Institute for Research and Advanced Studies-State University of Guayaquil respectively.

I have been fortunate in having some many friends during the last years since I left my country in 1991. Special thanks go to Dr. Arthur Gerstenfeld and his lovely wife Dr. Susan Vernon-Gerstenfeld for being our friends when living in Worcester. To Pastor

Mark Nevius and all the members of the First Alliance Church at Worcester, Massachusetts for their spiritual help and fellowship. When I came to Raleigh early 2000, I meet one of the more influential classmates in my student life, Dr. Joseph Gregory, who always have a smile and advise for all his lab mates when needed. God bless you Joe ...!!!

To Mr. Francisco Alvarez and his wife Mrs. Mela de Alvarez for all their loving support and friendship showed during the last three years. “Don Francisco”, thank you very much for showing me the way in finding the Lord Jesus Christ.

Special thanks go to Dr. Mark Norris for given me the opportunity to be part of Mechanical R&D Division at the Thomas Lord Research Center, Lord Corporation during the last year and Dr. Askari Badre-Alam for being my mentor meanwhile being at Lord.

From the bottom of my heart I want to thanks to my parents, Luis Carlos and Maria Adela, they always believed in me since my earlier student days, they saw in me perseverance, dedication and love for what I was doing...studying. All their prayers and hopes were not in vane. Dad, I don't know were are you now, but I just want to tell you, I made it!

I am especially in debt to my wife, Maria Esther, for her encouragement and abiding love. I am extremely blessed to have such a patience and supportive wife. Maria Esther

thanks for being with me in hard and good times of my life. Peri, thanks for following this dreamer in his adventure that has taken few years since we left our country looking for better life for our family. I was not wrong when I married you; you and my sons have been my inspiration for reaching my dream in getting a higher education. My sons Jhostyn and Steven, they given me much joy, energy and inspiration.

**“Perita” It took so long, but I made it!**

# TABLE OF CONTENTS

<b>List of Tables</b>	<b>ix</b>
<b>List of Figures</b>	<b>x</b>
<b>1 Introduction</b>	<b>1</b>
1.1 Motivation for the Study	2
1.2 Motivation for Trans-Permanent Magnetic Actuation	3
1.3 Technology Convergence	5
1.4 Overview of the Thesis	7
1.5 References	9
<b>2 Analysis of Trans-Permanent Magnetic Systems</b>	<b>12</b>
2.1 Introduction	13
2.2 Governing Equations	14
2.3 Experimental Set-Up and Results	19
2.4 Concluding Remarks	21
2.5 References	22
<b>3 Trans-Permanent Magnetic Valves Using Alternating Uniform Linear Stacks</b>	<b>40</b>
3.1 Introduction	41
3.2 Principles of Operation	42
3.3 Linear Stack Relationships	44

3.4	Alternating Uniform Linear Stacks	48
3.5	Valve-Spring Design	49
3.6	Control Circuit	51
3.7	Prototype Valve	52
3.8	Testing	54
3.9	Summary and Conclusions	56
3.10	References	58
<b>4</b>	<b>Recommendations</b>	<b>73</b>
4.1	Recommendations and Conclusions	74
4.1.1	General Recommendations	74
4.1.2	Conclusions and Recommendations Pertaining to Valves	75
4.1.3	Unanswered Questions	78
	<b>Appendix A: BasicX-24 Code</b>	<b>79</b>
	<b>Appendix B: BasicX-24 and L298 Connections</b>	<b>82</b>
	<b>Appendix C: Springs Test</b>	<b>84</b>

## LIST OF TABLES

<b>Table 2.1</b>	Magnetic Material Properties	37
<b>Table 2.2</b>	<i>T-PM</i> Design	38
<b>Table 2.3</b>	Circuit Parameters	39
<b>Table 3.1</b>	Circuit Specifications	68
<b>Table 3.2</b>	Magnetic Material and Coil Design	69
<b>Table 3.3</b>	Numbering of Gaps Combinations	70
<b>Table 3.4</b>	Test Results ( $k = 1.3 \text{ N/cm}$ )	71
<b>Table 3.5</b>	Test Results ( $k = 1.3 \text{ N/cm}$ , $p_0 = 15 \text{ psi}$ )	72

## LIST OF FIGURES

<b>Figure 2.1</b>	<i>T-PM</i> system	24
<b>Figure 2.2</b>	Geometry of the <i>T-PM</i> magnets	25
<b>Figure 2.3</b>	Two permanent magnets	26
<b>Figure 2.4</b>	Magnetization curve	27
<b>Figure 2.5</b>	The $R_oC/LRC$ charge and discharge circuits	28
<b>Figure 2.6</b>	Design process for <i>T-PM</i>	29
<b>Figure 2.7</b>	Experimental set-up	30
<b>Figure 2.8</b>	Comparison between predicted and measured force	31
<b>Figure 2.9</b>	Comparison between predicted $B$ -field and measured $B$ -field	32
<b>Figure 2.10</b>	Charge response of charging $R_oC$ circuit	33
<b>Figure 2.11</b>	Current response of charging $R_oC$ circuit	34
<b>Figure 2.12</b>	Charge response of discharging $LRC$ circuit	35
<b>Figure 2.13</b>	Current response of discharging $LRC$ circuit	36
<b>Figure 3.1</b>	<i>T-PM</i> system	60
<b>Figure 3.2</b>	Linear stack of magnets	61
<b>Figure 3.3</b>	Photo and schematic of control circuit	62
<b>Figure 3.4</b>	Measured force vs. gap curve (Alnico 5 and Ceramic 8)	63
<b>Figure 3.5</b>	Stack geometry	64
<b>Figure 3.6</b>	Magnet arrangements	65
<b>Figure 3.7</b>	Prototype valve	66
<b>Figure 3.8</b>	Design curve for valve spring	67

# **Chapter 1**

## **Introduction**

## 1.1 Motivation for the Study

The subject of magnetic actuation is very broad. It encompasses many technologies, a wide range of magnetic circuit topologies and performance characteristics, and an ever-increasing spectrum of applications in just about all of the market sectors [1.1]. Modern magnets are far more powerful than those of only few years ago, which have greatly increased their usefulness in a wide range of products [1.2]. Continuing developments in power electronics, microprocessors and digital control, and the growing demand for higher performance motion control systems, has created a research and development environment in the area of magnetic actuators that is probably more active than at any other time [1.3]. Actuator types and topologies are emerging with widely varying operational characteristics, in terms of displacement (rotary or linear), speed of response, position accuracy and duty cycle [1.4].

Permanent magnets date back to beginning of time and electromagnets date back hundreds of years; their behavior is well known. Permanent magnets do not require a supply of power to operate, but their field strength cannot be varied. In contrast, the field strength of electromagnets can be varied, but they require a continuous supply of power to operate. In many low-power applications it is desirable to achieve both of the advantages exhibited by permanent magnets and electromagnets simultaneously, namely, to maintain the ability to vary field strength and not to require a continuous supply of power.

Ideally, the question arises whether it is possible to vary the magnetic field strength; for example, to move to a mid-range condition. Current would be applied to the accompanying

electromagnetic coil to vary the magnetic field strength and to open the valve to some mid range level. Alternatively, another current could be applied to the coil to add to the magnetic field taking the device to a different range condition. The understanding of general principles by which a magnetic field can be changed on board and the development of devices that are based on these principles is the subject of this dissertation. In short, a method or procedure for switching the states of permanent magnets in real-time is sought. In this dissertation, this is called *trans-permanent magnetics (T-PM)*.

Through *T-PM* the hope is to create a method for fail-safe operation of devices that remain locked when power is not supplied. This could lead to new types of low power devices, to new devices with drastically reduced wear, and possibly to other advantages, not foreseen. This dissertation will show that *T-PM* systems are possible, although their design is not trivial.

## **1.2 Motivation for Trans-Permanent Magnetic Systems**

The motivation for the study of *T-PM* systems relies on the advantages exhibited by permanent magnets and electromagnets simultaneously, namely, the ability of a permanent magnet to create a force when no power is supplied and the ability of an electromagnet to provide a varying level of force.

There are many methods for magnetizing hard materials. Perhaps, the most common method used in the manufacture of permanent magnets is the pulse magnetization process. This

procedure is done by an off-board process by means of an open magnetic circuit, partially open circuit or in circuit closed by a core [1.5]. Papers concerned with pulse magnetization of permanent magnets are scarce [1.6, 1.7, 1.8, 1.9, 1.10].

The discharging of a capacitor bank through an inductance coil can be described in a simplified way by means of a single ordinary differential equation. Temporal behavior of current flowing in the on-board magnetizer circuit is affected by the specific values of the circuit parameters and their mutual relations. In order to achieve values that saturate the permanent magnet, the following requirements must be satisfied: the duration of the current pulse, the peak current time, and the peak current density in the magnetizing winding. Those relationships are developed in Chapter 2.

The states of soft permanent magnetic materials can be changed by varying the magnetic field strength in real-time by an on-board magnetization process [1.11, 1.12]. Control terminology, the permanent magnet provides regulation (holding the state) and the electromagnets provide tracking (changing the state). The state is changed by varying the magnetic field intensity of a tunable permanent by an on-board process [1.1, 1.2]. The following combinations of properties are potentially achievable:

1. *Soft Locking*: Forces between permanent magnets elastically maintain the states.
2. *Zero-Power Hold*: In many applications, regulation is a continuous operation and tracking is intermittent. The *T-PM* consumes no power during regulation because the hold states are

maintained by permanent magnets [1.12]. This can reduce power requirements by several orders of magnitude.

3. *Multiple Equilibrium Settings*: This dissertation will show that a *T-PM* valve can be designed to possess a set of equilibrium positions (state combinations) depending on the number of permanent magnets employed. The theoretical number of combinations is shown in Chapter 3 to be  $M = 2^{\text{int}\left(\frac{n+1}{2}\right)}$  where  $n$  is the number of magnets.

4. *Low Wear and High Reliability*: Mechanical wear in a *T-PM* should be inherently low since the electromagnets are turned off most of the time, depending on the application.

### 1.3 Technology Convergence

The author has not found trans-permanent magnetic systems, as they were conceived in this dissertation, either in the research literature or as commercial products in catalogs. Therefore, they represent a new research and development area. The advantages of *T-PM* technology it make easy to visualize a spectrum of possible applications. Like many other new devices, the convergence of relatively new technologies has enabled the *T-PM* system technology to become practical. The *T-PM* technology requires solid-state relays that can operate with a maximum supply voltage of 46 V and switch large currents up to 4 A in continuous operation [1.13], electrochemical super-capacitors that hold a very high charge that can be released very quickly, and take up very little space – all of which could be realized only recently.

These super-capacitors provide the energy needed for the *T-PM* pulse coil magnetization [1.14].

Another enabling advancement is clearly the advent of microcontrollers that interface with machines rather than people, eliminating the need for monitors, keyboards, or any other devices that require human interaction. Microcontrollers are very inexpensive compared to the price of the final system [1.15]. The latest development of miniature wireless sensors and data acquisition systems will also play a role [1.16]. These tiny devices can be placed within implants, on spinning machinery, and within composite materials. Because they can tolerate extremely high *G* levels and high temperatures, sensor measurements can be made in applications where previously no data could be obtained. With these miniature sensors batteries are eliminated which means that the embedded sensors can be queried for the life of the structure. Significantly, development work is being conducted to increase the energy density of permanent magnets [1.17]. Other advancements are associated with better magnetic field modeling codes [1.18, 1.19, 1.20]. A recent NASA development, the Super Ni-Cd Spacecraft Battery, could enable *T-PM* systems to be used in large aperture surface deployment applications [1.21]. The convergence of technology creates possibilities that *T-PM* systems and the necessary support equipment could become more efficient than PM motors, proportional valves, etc.

## 1.4 Overview of the Thesis

This dissertation contains two papers. Chapter 2 contains the first paper entitled “*Analysis of Trans-Permanent Magnetic Systems.*” It focuses on the development of a method for switching the states of permanent magnets through an on-board magnetization process. That paper describes the governing equations needed for the analysis and the design tools of *T-PM* systems. This paper also demonstrates their feasibility experimentally. In doing so, the paper presents a method that has the potential of leading to new low power designs for electromechanical devices. That paper appears in the Journal of Dynamic Systems, Measurement and Control.

Chapter 3 contains an edited version of a second paper entitled “*Trans-Permanent Magnetic Valves Using Alternating Uniform Linear Stacks.*” that was submitted for publication in a technical journal. This paper extends the developments of the first paper to the application of low-power valve control. Whereas a conventional approach to low power valve control would be based on latching mechanisms that turn off valves during inactive periods, this paper describes an approach that potentially eliminates the need for such latching mechanisms. Instead of latching mechanisms, the principles of *T-PM* are employed to switch the states of permanent magnets; the use of permanent magnets instead of electromagnets eliminates power loads during inactive periods, thereby reducing power consumption to low levels. For example, a new class of solenoid valves (See “Next Generation Solenoids Draw Less Power and Produce More Force,”

[www.machinedesign.com/ASP/stArticleID/55020/strSite/MDSite/viewSelectedArticle.asp](http://www.machinedesign.com/ASP/stArticleID/55020/strSite/MDSite/viewSelectedArticle.asp)) draws about 10 Watts of power during continuous operation. The *T-PM* valve would draw a comparable amount of power only during the periods when the capacitors are being charged, which could be as low as 0.01% of the time of continuous operation or lower, depending on the manner in which the *T-PM* valve is used. The *T-PM* actuator that is operated 0.01% of the time consumes about 10,000 times less power than the conventional 10 Watt valve.

The magnets in a *T-PM* valve are configured in a stack. The relationships between the strength and number of permanent magnets in the stack and the stroke and resolution of the valve are developed. Then the paper reports on the design and testing of a prototype valve that uses an alternating uniform linear stack. The paper shows that the alternating uniform linear stack is well suited for digital process valves having a small number of states in contrast with digital regulating valves that have a large number of states. This paper finds that trans-permanent valve represents a promising valve actuation technology.

## 1.5 References

- 1.1 Howe, D., 2000. "Magnetic Actuators", *Sensors and Actuators*, 81, pp. 268-274.
- 1.2 Oersted Technology II, Inc., 2001 ([www.oersted.com](http://www.oersted.com))
- 1.3 Churn, P.M., Pia, Z.P., Mellor, P.H., and Howe, D., 1997. "The Benefits of Direct Drive Linear Actuation in Point-to-Point Material Transportation in Packaging Applications", *Proceedings of the PCIM*, pp. 65-74.
- 1.4 Raimondi, G.M., McFarlane, R.D., Binham, C.M., Atallah, K., Howe, D., Mellor, P.H., Capewell, R., and Whitney, C., 1998. "Large Electromechanical Actuation Systems for Flight Control Surfaces", *IEE Colloquium on All-electric Aircraft*, pp. 24-35.
- 1.5 Zycki, Z., 1995. "Experimental Design of Permanent Magnet Demagnetization Curve using Approximated Equations", *COPEL-The International Journal for Computation and Mathematics in Electrical and Electronic Engineering*, 14(4), pp. 303-308.
- 1.6 Steingroever, E., and Ross, G., 1993. Magnetization, Demagnetization and Calibration of Permanent Magnet Systems, Magnet Physik, Koeln.

- 1.7 Zycki, Z., and Rudnicki, M., 1995. "Heat Dissipation in Pulse Magnetization of Permanent Magnets", Proceedings 8<sup>th</sup> International Symposium on Theoretical Electrical Engineering, Thessaloniki, pp. 82-85.
  
- 1.8 Zycki, Z., and Pawluk, K., 1998. "Design of RLC Circuit for Pulse Magnetizer of Permanent Magnets", COPEL-The International Journal for Computation and Mathematics in Electrical and Electronic Engineering, 17(1,2,3), pp. 412-417.
  
- 1.9 Zycki, Z., and Pawluk, K., 1997. "Pulse Magnetizing Process and Evaluation of the Final Stage of Permanent Magnets", Electromagnetic Fields in Electrical Engineering, A. Krawczyk and S.Wiak (eds), IOS Press, pp. 555-558.
  
- 1.10 Andrejevskiy, E.A., Nepokritiyi, L.N., and Miheyeva, L.N., 1968. "Analysis of Parameters of a Pulse Magnetization System", Kontrolno-Izmieritel'naya Technika, 4, pp. 59-65.
  
- 1.11 Silverberg, L and Duval, L, 2003, "Analysis of Trans-Permanent Magnetic Systems", Journal of Dynamic Systems, Measurement and Control, 125(3), pp 146-151.
  
- 1.12 Judy, J.W., Yang, H., Myung, N.V., Yang,C.K., Schwartz, M., and Kobe, K. 2000 "Integrated Ferromagnetic Micro-sensors and Micro-actuators", Proceedings of the Fifth International Symposium on Magnetic Materials, Process and Devices, 198<sup>th</sup>

- Meeting of the Electromechanical Society, Phoenix, AZ, October 22-27, 2000, pp 456-468.
- 1.13 L298 Dual Full Bridge Driver. STMicroelectronics ([www.st.com](http://www.st.com))
- 1.14 Report of the Marshall Space Flight Center 1993 Phase II: Electrochemical Super Capacitors for Electromechanical Actuators.
- 1.15 NetMedia Inc., Manufacturer of BasicX-24 Microprocessor. ([www.netmedias.com](http://www.netmedias.com))
- 1.16 EmbedSense™ Wireless Sensor, MicroStrain Microminiature Sensors, 2003
- 1.17 Magnetic Materials Catalog 2003. Dura Magnetics, Inc., Sylvania, OH.
- 1.18 ANSYS Emag™, Electromagnetic Simulation Software.
- 1.19 Maxwell SV®, Electromagnetic Field Simulation Package, Ansof Corporation.
- 1.20 FEMM Finite Element Method Magnetics, 2003
- 1.21 Super Ni-Cd Spacecraft Battery Handling and Storage Practice, NASA Tech Briefs, May 2003.

## **Chapter 2**

### **Analysis of Trans-Permanent Magnetic Systems**

## 2.1 Introduction

Permanent magnets and electromagnets date back hundreds of years; their behavior is well known. Permanent magnets do not require a supply of power to operate, but their strength cannot be varied. In contrast, the strength of electromagnets can be varied, but they require a continuous supply of power to operate. In many low-power applications it is desirable to achieve both of the advantages exhibited by permanent magnets and electromagnets simultaneously, namely, to maintain the ability to vary strength and not to require a continuous supply of power. This paper introduces a method for achieving these advantages using *trans-permanent magnetic (T-PM) systems*. Several of the potentially beneficial *T-PM* applications are valves, force actuators, and displacement actuators. In these applications the system can be held in one state or another (opened or closed) for an indefinite period of time without consuming power or fuel or experiencing significant wear. Flow valves can be held open for months at a time during which flow is allowed to continue. The surface of a spacecraft antenna can be reconfigured to optimize throughput and held in position for years. Shut-off dampers in HVAC ducts can be held open throughout a season.

The *T-PM* has the potential of leading to simpler designs of dynamic systems in these and in other applications by eliminating the need for latching mechanisms that would otherwise be required in order to achieve the same low-power characteristic.

*T-PM* systems are composed of four basic parts: a tunable permanent magnet, a non-tunable permanent magnet, a coil, and an *LRC* circuit (Fig. 2.1). Varying the strength of the tunable

permanent magnet - through magnetization, varies the force between the tunable permanent magnet and the non-tunable permanent magnet. The tunable permanent magnet is magnetized by creating a large short-duration electromagnetic field around the tunable magnet, which in turn is created by a large short-duration current that is produced from a discharging *LRC* circuit. Note that large, short-duration magnetizing pulses are already used for off-board magnetization [2.1], and a similar approach will be used in this paper for on-board magnetization.

This paper demonstrates the feasibility of *T-PM* systems and develops the needed design and analysis tools. Section 2.1 describes the equations that govern the force between permanent magnets with rectangular cross-sections, shows how the magnetization curve is used, and then develops the needed relationships associated with the *LRC* circuit. Section 2.3 describes an experimental set-up that was developed in order to verify the feasibility of *T-PM* systems, and presents experimental results and analytical predictions. Section 2.4 concludes the paper.

## 2.2 Governing Equations

Consider two permanent magnets with rectangular cross-sections, as shown in Fig. 2.2. An efficient method of calculating the force between the two magnets when the two magnets are identical to each other was developed in [2.2]. It is rather easy to extend these results to permanent magnets that are different [2.3]. The force between two different permanent magnets is

$$F = \frac{\mu_0}{4\pi} M_1 M_2 \left[ \frac{\pi R^2}{N_r N_\theta} \right]^2 N_\theta \sum_{m=0}^3 \sum_{i=1}^{N_r} \sum_{j=1}^{N_r} \sum_{k=1}^{N_\theta} \frac{\delta h_m}{[r_i^2 + r_j^2 - 2r_i r_j \cos(\theta_k) + h_m^2]^{3/2}} \quad (2.1)$$

where

$$h_m = \begin{cases} h & \text{if } m = 0 \\ h + t_1 & \text{if } m = 1 \\ h + t_2 & \text{if } m = 2 \\ h + t_1 + t_2 & \text{if } m = 3 \end{cases}, \quad \delta = \begin{cases} 1 & \text{if } m = 0 \\ -1 & \text{if } m = 1 \\ -1 & \text{if } m = 2 \\ 1 & \text{if } m = 3 \end{cases}$$

in which  $N_r$  and  $N_\theta$  denote the number of radial and circumferential divisions in the discretization,  $\mu_0 = 4\pi \times 10^{-7}$  Wb/Am is the magnetic constant of free space,  $M_1$  is the magnetization in the tunable magnet,  $M_2$  is the magnetization in the non-tunable magnet,  $h$  denotes the gap,  $t_1$  denotes the thickness of the tunable magnet,  $t_2$  denotes the thickness of the non-tunable magnet, and  $R$  denotes the radius of the tunable magnet, which is equal to the radius of the non-tunable magnet (Fig. 2.3). Equation (2.1) assumes that the magnetization is constant throughout the inside of each magnet. The flux density normal to the surface between the two magnets is

$$B = \sqrt{\frac{2\mu_0 F}{A}} \quad (2.2)$$

where  $F$  is the magnetic force between the magnets, given in Eq. (2.1), and  $A$  is the cross-sectional area between the magnets [2.4].

The magnetization of the tunable magnet is governed by the magnetization curve of the form shown in Fig. 2.4 [2.1]. In the case of the *T-PM*, the *B*-axis refers to the permanent field of the tunable magnet and the *H*-axis refers to the short-duration electromagnetic field created by the short-duration current produced from the discharging *LRC* circuit. Let the initial state of the tunable magnet be located at either point  $(0 B_r)$  or point  $(0 -B_r)$ , depending on whether the interior surface is initially North or South. A short-duration field greater than or equal to  $H_C$  causes the permanent field to move from point  $(0 B_r)$  to point  $(-H_C 0)$  or from point  $(0 -B_r)$  to point  $(H_C 0)$ . Note that the strength of the permanent field of the non-tunable magnet is not altered by the short-duration electromagnetic field whether or not it is in close proximity to the electromagnetic field. The strength of the permanent field of the non-tunable magnet is not altered because the non-tunable magnet is a "hard" magnet that requires a higher level of magnetization than is applied to the tunable magnet, which is a "soft" magnet.

The short-duration electromagnet field created by the current in the coil of wire is

$$H = \frac{N i_m}{l_0} \quad (2.3)$$

where  $i_m$  is the maximum current in the coil,  $N$  is the number of turns, and  $l_0$  is the length of the coil [2.6].

The purpose of the *LRC* circuit is to store charge and to discharge it into the coil (Fig. 2.5).

The left loop of the circuit charges the capacitor and the right loop discharges the capacitor.

The discharging *LRC* circuit is governed by

$$L\ddot{q} + R\dot{q} + \frac{1}{C}q = V \quad (2.4)$$

in which  $L$  denotes the inductance in the coil,  $R$  denotes the discharge resistance of a circuit resistor,  $C$  denotes the capacitance of the storage capacitor,  $q$  denotes charge,  $V$  denotes an applied  $DC$  voltage, and over-dots denote time-differentiation [2.7]. The effect of inductor non-linearity is neglected; this is justified later by the close agreement between the measurements and the predictions, although it cannot be concluded that inductor non-linearity can be neglected in other configurations. By closing the switch, current is discharged through the coil over a period of time  $T$ . The discharge time  $T$  must be larger than the internal settling time  $T_i$  associated with the molecular vibration in the tunable magnet during the magnetization [2.5]. The response of the circuit was over-damped for the range of parameters selected in the experimental set-up. The over-damped response is (open circuit)

$$q = CV_0 \left[ \frac{\alpha + \beta}{2\beta} e^{(-\alpha + \beta)t} + \frac{-\alpha + \beta}{2\beta} e^{(-\alpha - \beta)t} \right], \quad (2.5a,b)$$

$$\beta = \alpha \sqrt{1 - \left( \frac{\omega}{\alpha} \right)^2}$$

in which  $CV_0$  denotes the stored charge in the capacitor,  $\alpha$  is the mean decay rate, and  $\omega$  is the undamped frequency of the circuit, given by

$$\alpha = \frac{R}{2L}, \quad \omega = 1/\sqrt{LC}. \quad (2.6a,b)$$

Define the discharge time  $T$  of the circuit as the time required to remove 99% of the charge from the capacitor. The discharge time can be obtained in closed-form from Eq. (2.5) for  $\omega/\alpha \ll 1$  by neglecting the rapidly decaying component  $e^{(-\alpha-\beta)t}$  of the response, to get

$$T = \frac{1}{-\alpha + \beta} \ln \left[ \frac{1}{100} \frac{2\beta}{\alpha + \beta} \right] \quad (2.7)$$

Also, from Eq. (2.5), the maximum current  $i_m$  and the time  $t_m$  of the maximum current are obtained in closed-form,

$$i_m = CV_0 \frac{\alpha^2 - \beta^2}{2\beta} \left[ \left( \frac{\alpha + \beta}{\alpha - \beta} \right)^{\frac{-\alpha + \beta}{2\beta}} - \left( \frac{\alpha + \beta}{\alpha - \beta} \right)^{\frac{-\alpha - \beta}{2\beta}} \right] \quad (2.8a.b)$$

$$t_m = \frac{1}{2\beta} \ln \left[ \frac{\alpha + \beta}{\alpha - \beta} \right]$$

From Eqs. (2.7) and (2.8) the ratio of the time of the maximum current and the discharge time is

$$\frac{t_m}{T} = \frac{\alpha - \beta}{2\beta} \frac{\ln \left[ \frac{\alpha + \beta}{\alpha - \beta} \right]}{\ln \left[ 100 \frac{\alpha + \beta}{2\beta} \right]} \quad (2.9)$$

This analysis suggests a relatively easy design process for the  $T$ -PM (Fig. 2.6). The design process can begin with a desirable force-gap pair  $(F, h)$  in Eq. (2.1). The force-gap pair

characterizes the mechanical work that can be done by the  $T\text{-}PM$ . The  $B$ -field required to achieve the desired  $(F, h)$  pair is determined in the coil design from Eq. (2.2). The  $H$ -field required in the electromagnet to achieve the required  $B$ -field is determined from the magnetization curve. The maximum current  $i_m$  in the coil to achieve the needed  $H$ -field is determined from Eq. (2.3). The  $LRC$  parameters for the discharging that are required in order to achieve the needed maximum current and the needed settling time are determined from Eqs. (2.7) and (2.8). The time constant  $T$  is bound from below by an internal settling time  $T_i$  associated with the molecular vibration in the tunable magnet during magnetization. The  $LRC$  circuit is driven by a power supply.

### 2.3 Experimental Set-Up and Results

The  $T\text{-}PM$  concept is reduced to practice in the following set up (Fig. 2.7). A ceramic magnet having a relatively high coercivity was selected for the non-tunable (hard) permanent magnet (Dexter Magnetic Technologies P253, [2.8]) and an Alnico magnet having relatively low coercivity was selected for the tunable (soft) permanent magnet (Dexter Magnetic Technologies P61C0250B, [2.8]) as shown in Table 2.1. The saturation induction  $B_s$  of the non-tunable magnet is 2346 G and the saturation induction of the tunable magnet is 13056 G. Notice that remanence is inversely proportional to coercivity. Before evaluating the performance of the  $T\text{-}PM$  system, the selected parameters were verified experimentally.

The force between the magnets was determined two ways. First, the force was predicted from Eq. (2.1) given levels of magnetization  $M_1$  and  $M_2$  that were specified by the vendor (Fig.

2.3). Then, the force was measured using a scale. Figure 2.8 compares the predicted force versus the gap with the measured force versus the gap. The predicted force was also substituted into Eq. (2.2) to yield a predicted  $B$ -field. The predicted  $B$ -field and the  $B$ -field measured using a Hall-effect sensors are compared in Fig. 2.9. The Hall-effect sensor was placed at the center of the magnets in the middle of the gap. The agreement between the predictions and the measurements is on the order of the measurement resolution. The error between the measured and predicted force was 4.9% and the error between the measured and predicted  $B$ -field was 5.5%.

The diameter and length of the tunable permanent magnet dictated the parameters of the coil except the number of turns. From Eq. (2.3), holding  $H$  constant, the number of turns is inversely proportional to the maximum current discharged into the coil. The number of turns was selected to be 350. The coil, armature, and permanent magnetic material parameters are shown in Table 2.2. The required maximum current in the coil was determined from Eqs. (2.7) and (2.8). Toward this end, an  $R_0$ ,  $R$ , and a  $C$  in the  $LRC$  circuit needed to be selected. The selected parameters are shown in Table 2.3. Notice that the discharge time is  $T = 0.4526$  sec (safely above  $T_i$ ), and the  $DC$  input voltage to the circuit was conveniently set to  $V = 12$  Volts. The resistance  $R$  and the capacitance  $C$  were determined from Eqs. (2.5b), (2.6a,b), (2.7) and (2.8a).

The charge and current across the capacitor during the charging of the capacitor are shown in Fig. 2.10 and 2.11 respectively. Since the charging of the capacitor and the discharging of the capacitor are performed in different parts of the circuit using different resistors, the time constants associated with the charging and the discharging are determined independently.

The charge and current across the discharging capacitor are shown in Fig. 2.12 and 2.13. Notice the rapid rise time of the current and the relatively slow settling time that is characteristic of the over-damped response, and that enables the maximum current achieved to be sufficiently large to create a sufficiently large  $B$ -field for the magnetization.

## 2.4 Concluding Remarks

This paper introduced an on-board method of switching the states of permanent magnets. The resulting dynamic systems were referred to as trans-permanent magnetic systems. The analysis tools for the design of trans-permanent magnetic systems were first developed. Then, the feasibility of these systems was demonstrated successfully in an experiment. Discharge times that were on the order of one second are achievable using coils surrounding a magnet that has a relatively small number of turns and using capacitors in the range of 0.02 Farads. It is concluded from these experiments that trans-permanent magnetic systems offer great promise in the design and development of low-power devices.

## 2.5 References

- 2.1 Zycki, Z. and Pawluk, K., 1998, "Design of RLC Circuit for Pulse Magnetizer of Permanent Magnets," International Journal for Computation and Mathematics in Electrical and Electronic Engineering, 17(1,2,3), pp. 412-417.
- 2.2 Furlani, E. P., 1993, "A Formula for the Levitation Force Between Magnetic Disks," IEEE Transactions on Magnetics, 29(6), pp. 4165-4169.
- 2.3 Furlani, E. P., 2001, Permanent Magnet and Electromagnetic Devices: Materials, Analysis, and Applications, Academic Press, New York.
- 2.4 Moon, F., 1984, Magneto-Solid Mechanics, John Wiley and Sons, New York.
- 2.5 Parker, R. J., 1990, Advances in Permanent Magnetism, John Wiley, New York.
- 2.6 Heck, C., 1974, Magnetic Materials and their Applications, Crane, Russak and Company, Inc., New York.
- 2.7 Scanlan, J.O. and Levy, R., 1970. Circuit Theory. Oliver and Boyd Publisher, Edinburgh.

2.8 Dexter Magnetic Technologies, Inc., Elk Grove Village, Illinois, 2001,  
([www.dextermag.com](http://www.dextermag.com)).

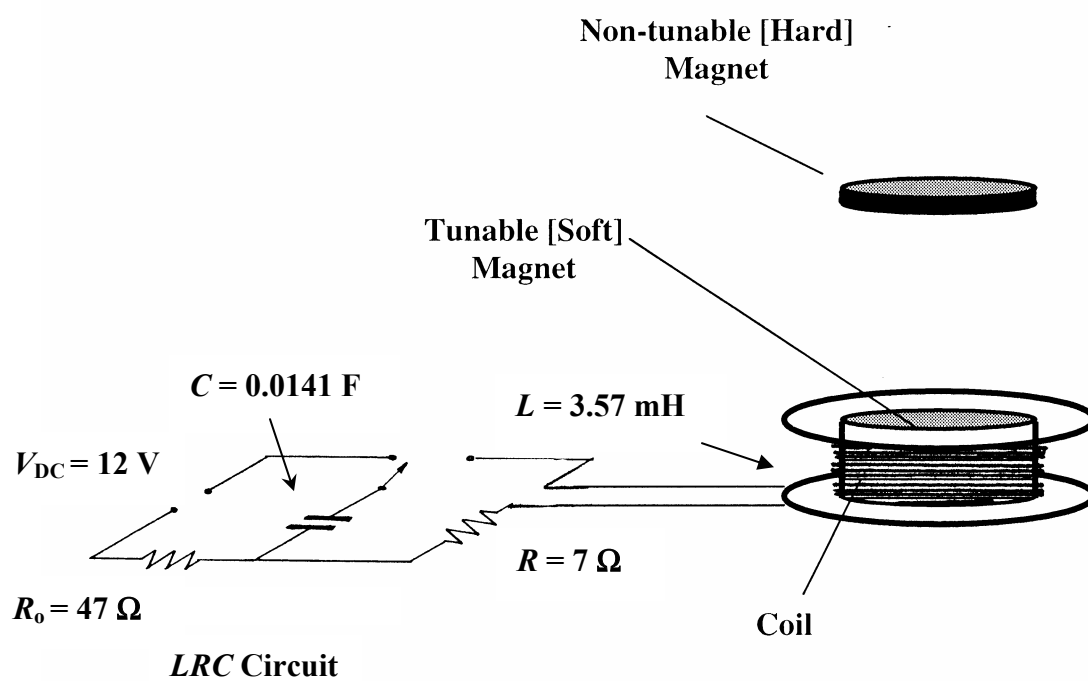
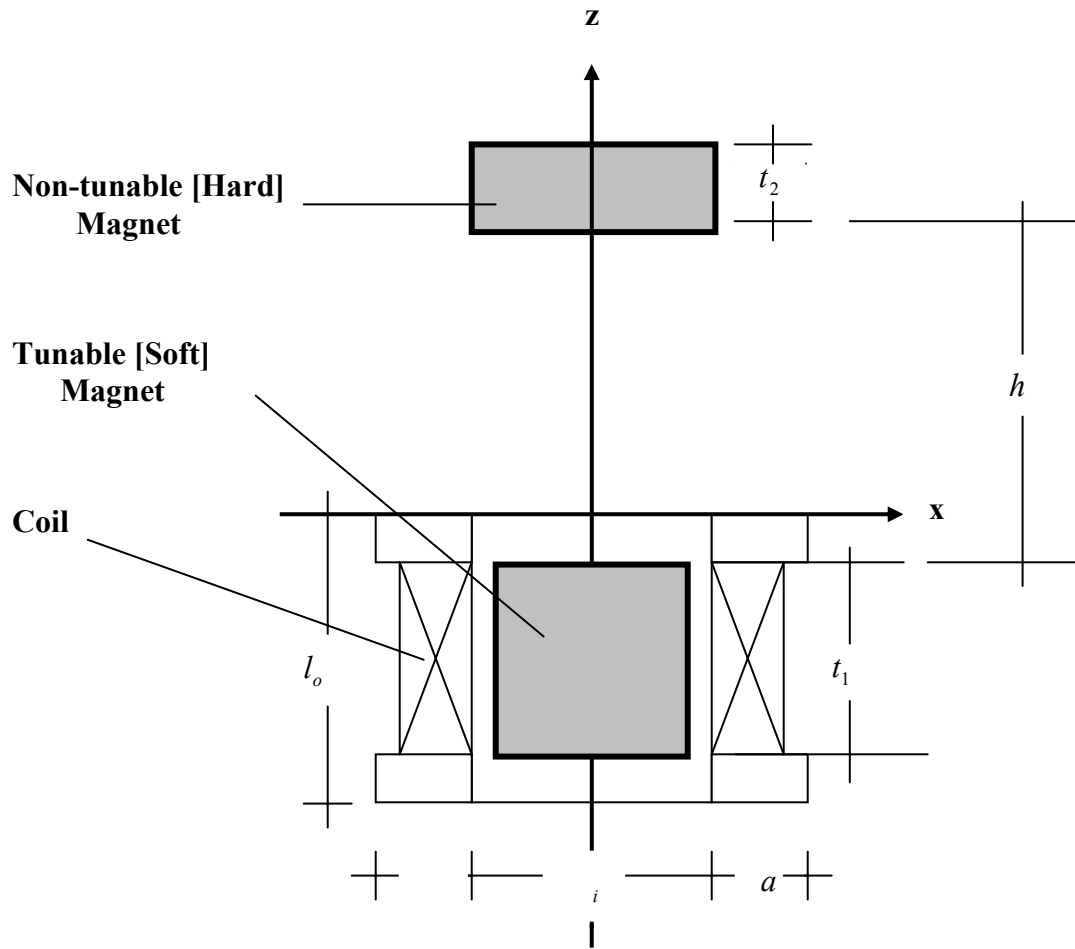
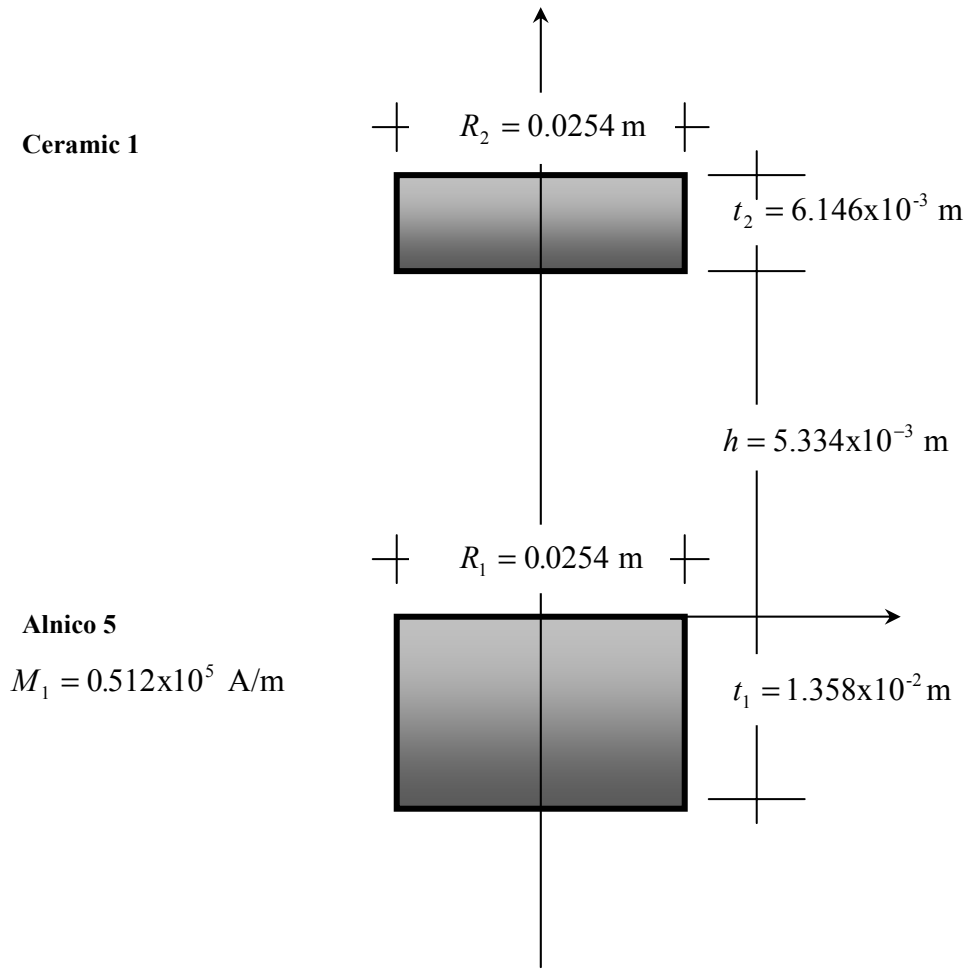


Figure 2.1 *T-PM* System



**Figure 2.2** Geometry of the *T-PM* magnets



**Figure 2.3 Two permanent magnets**

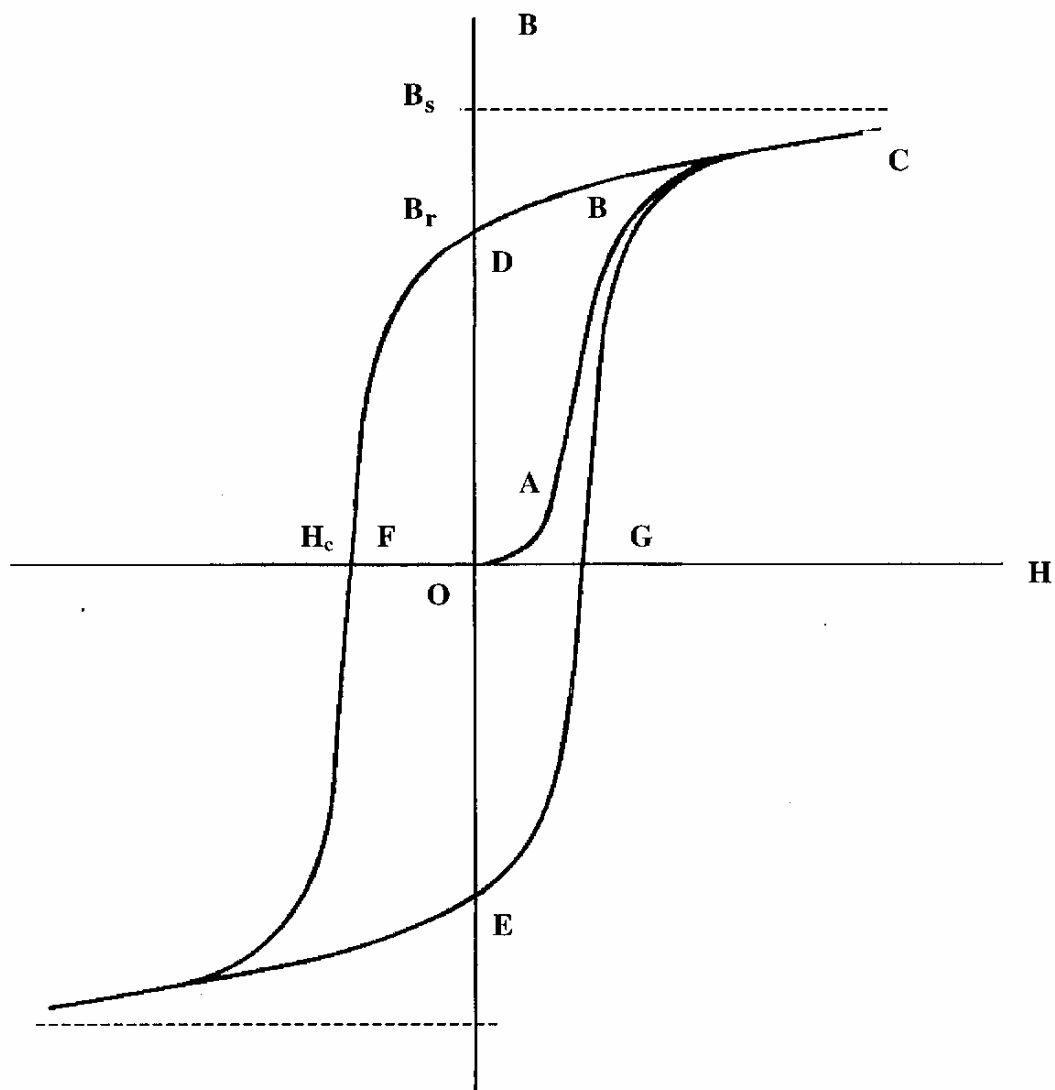
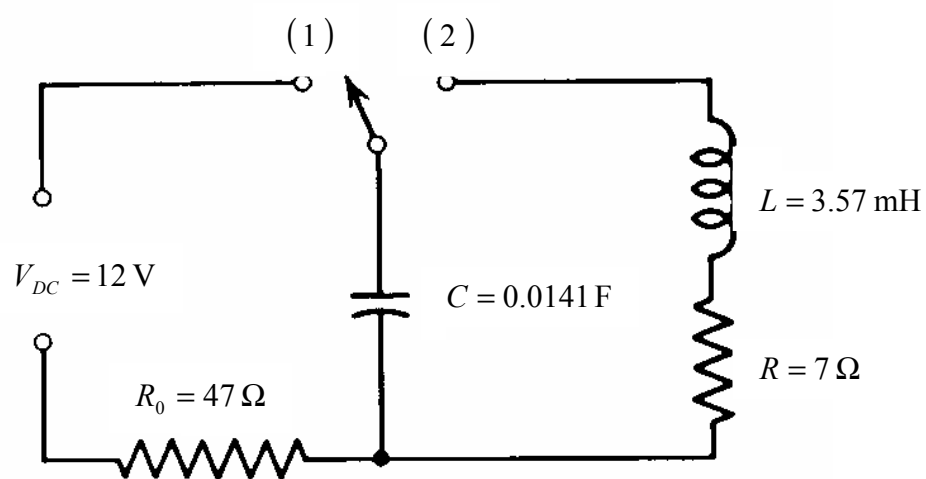
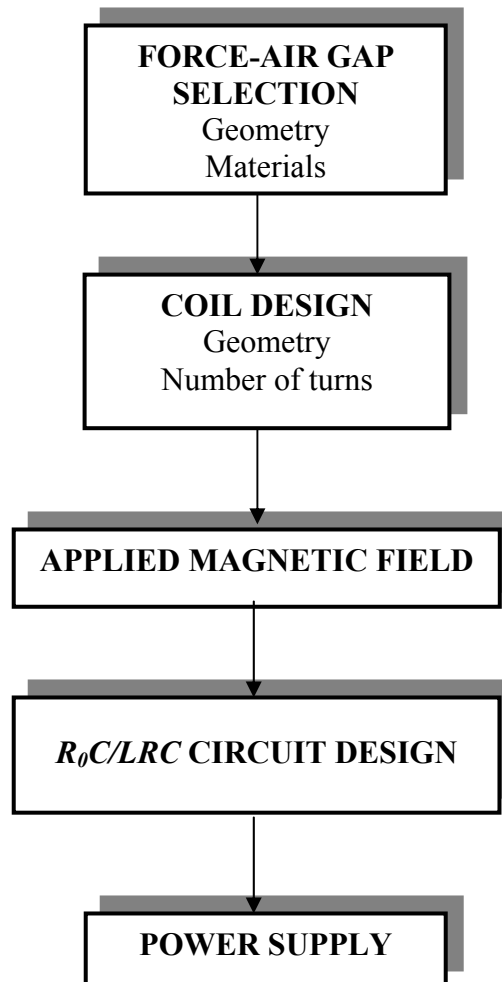


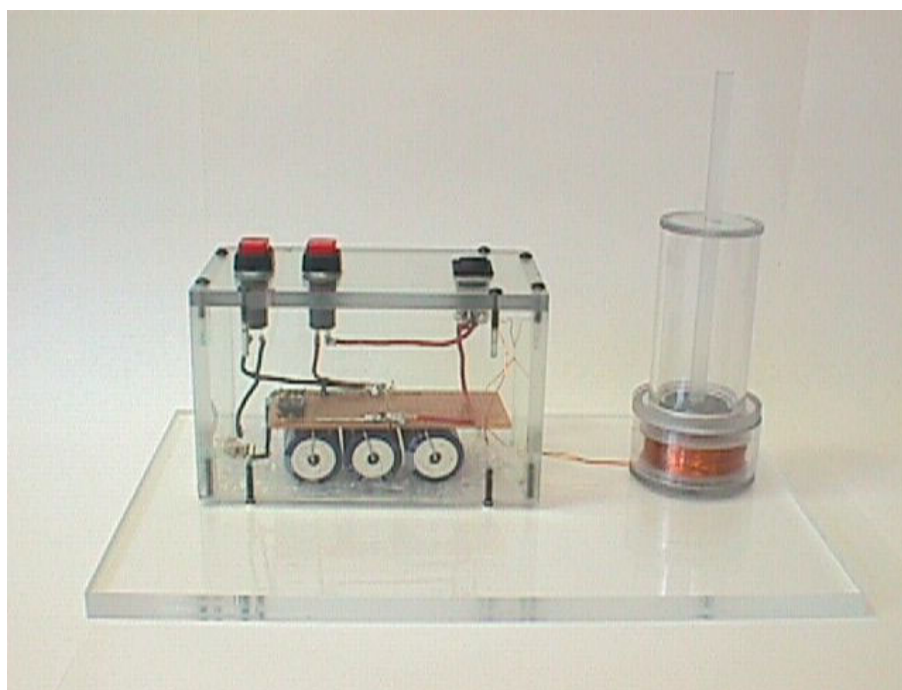
Figure 2.4 Magnetization curve



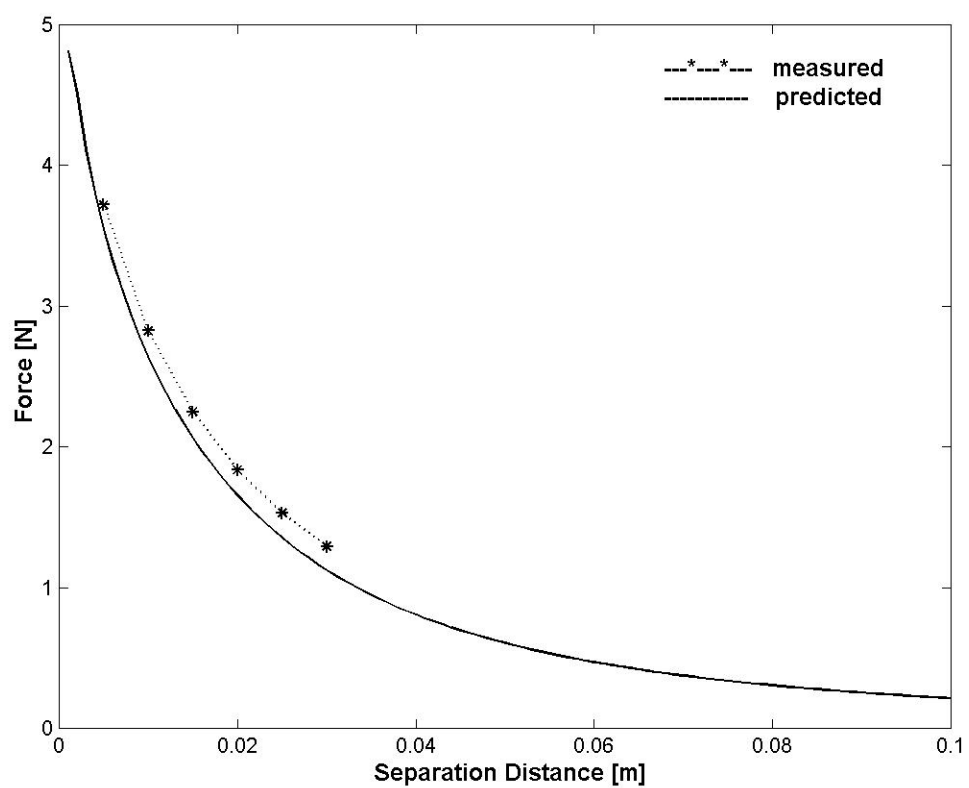
**Figure 2.5** The  $R_0C/LRC$  charge and discharge circuits



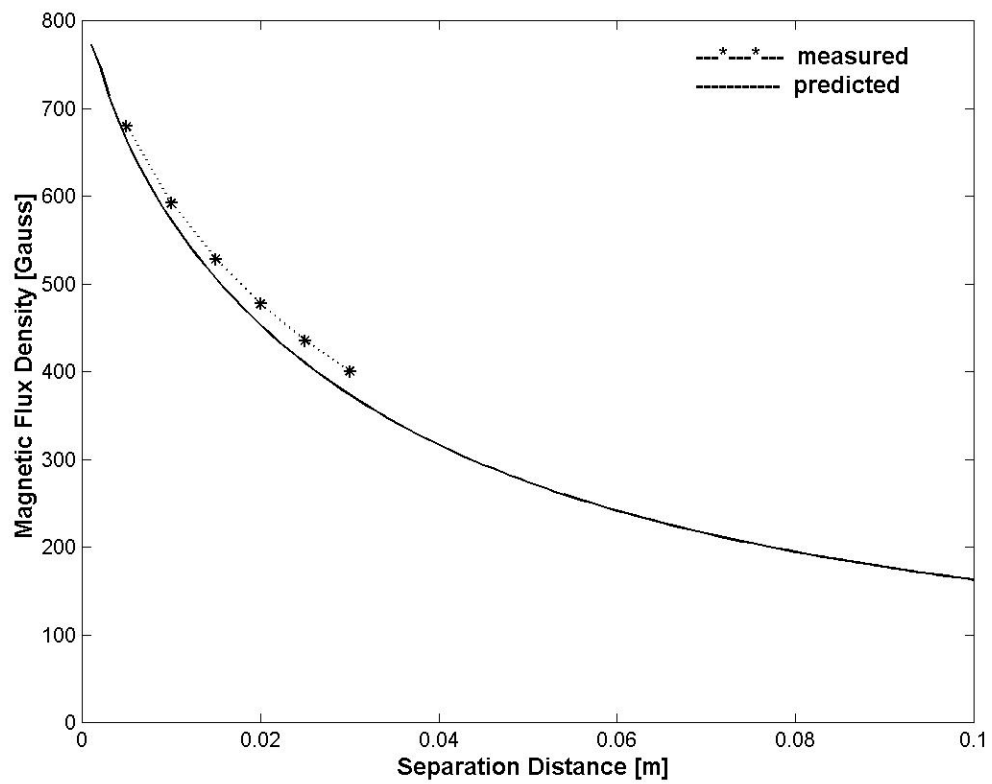
**Figure 2.6** Design Process for *T-PM*



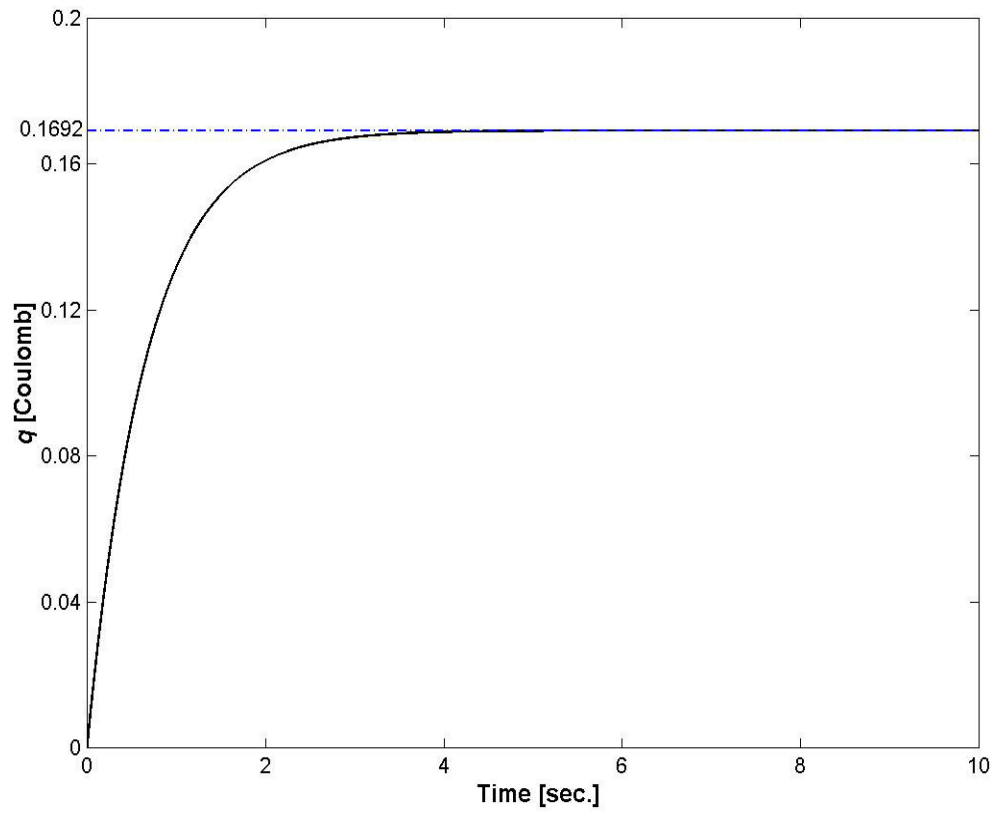
**Figure 2.7** Experimental Set-up



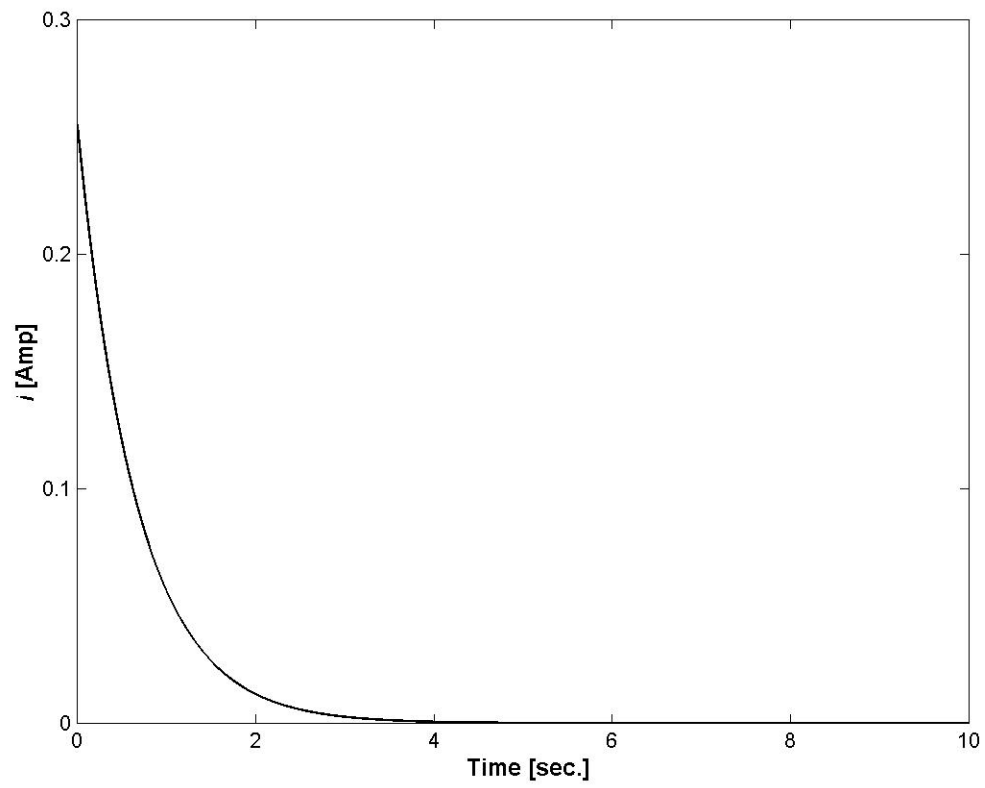
**Figure 2.8** Comparison between predicted and measured force



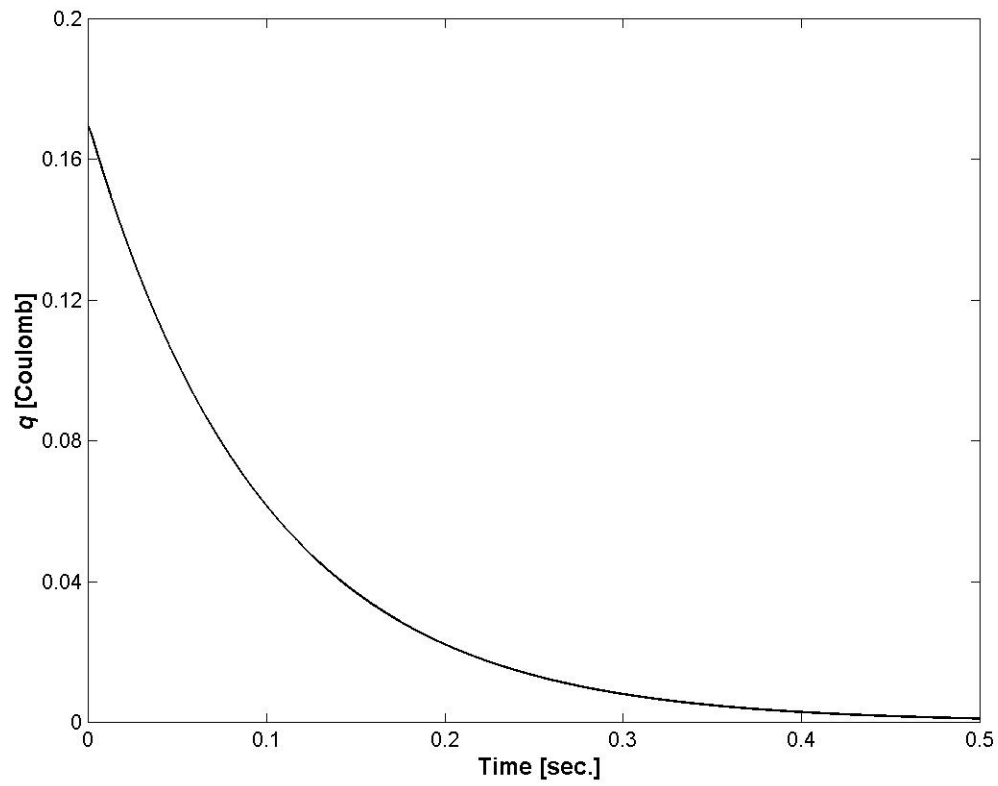
**Figure 2.9** Comparison between predicted  $B$ -field and measured  $B$ -field



**Figure 2.10** Charge response of charging  $R_0C$  circuit



**Figure 2.11** Current response of charging  $RC$  circuit



**Figure 2.12** Charge response of discharging *LRC* circuit

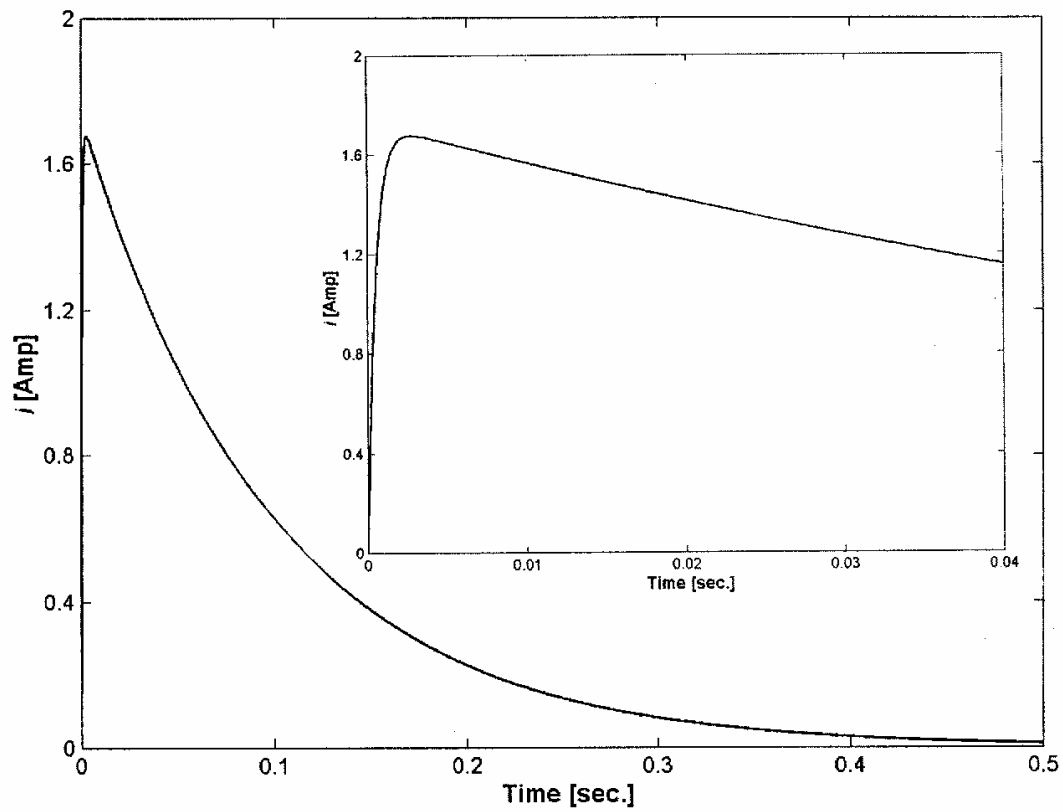


Figure 2.13 Current response of discharging *LRC* circuit

Table 2.1 Magnetic Material Properties

	Ceramic 1	Alnico 5
<b>Residual Magnetization</b> $B_r$	<b>0.23 T</b>	<b>1.24 T</b>
<b>Coercivity Force</b> $H_c$	<b>147 kAm<sup>-1</sup></b>	<b>50.9 kAm<sup>-1</sup></b>
<b>Intrinsic Coercivity Force</b> $H_{ci}$	<b>259 kAm<sup>-1</sup></b>	<b>54.1 kAm<sup>-1</sup></b>
<b>Energy Product</b> $BH_{\max}$	<b>8.36 kJm<sup>-3</sup></b>	<b>43.8 kJm<sup>-3</sup></b>

Table 2.2 *T-PM* Design

Armature	Mean diameter of coil $D$ , in Width of coil $l_o$ , in Inner diameter of coil $ID$ , in Outer diameter of coil $OD$ , in Mass $M$ , lb	1.525 0.635 0.975 1.75 0.0154
Magnets	<u>Alnico 5:</u> Diameter $\Phi_1$ , in Thickness $t_1$ , in Volume $V_1$ , in <sup>3</sup>  <u>Ceramic 8:</u> Diameter $\Phi_2$ , in Thickness $t_2$ , in Volume $V_2$ , in <sup>3</sup>	1.0 0.535 0.4202  1.0 0.242 0.19
Coil	Number of turns $N$ Type of Wire Inductance $L$ , H Resistance $R$ , $\Omega$	350 26 AWG $3.57 \times 10^3$ 7
Air gap	Length $h$ , in	0.21

**Table 2.3 Circuit Parameters**

	Nominal Values
<b>Resistance <math>R_o, \Omega</math></b>	<b>47</b>
<b>Capacitance <math>F</math>, Farads</b>	<b>0.0141</b>
<b>Inductance <math>L</math>, H</b>	<b><math>3.57 \times 10^3</math></b>
<b>Inductor resistance <math>R, \Omega</math></b>	<b>7</b>
<b>Power Supply [DC] <math>V_o</math>, Volts</b>	<b>12</b>

## **Chapter 3**

# **Trans-Permanent Magnetic Valves Using Alternating Uniform Linear Stacks**

### 3.1 Introduction

The development of digital process valves and digital regulating valves is of growing interest in the industry. Digital control, power-reduction, reliability, and speed are among the parameters that need to be improved [3.1, 3.2]. This chapter focuses on actuation improvements aimed at drastically reducing power consumption and wear. The approach that has been adopted in this paper is to apply recent developments in *T-PM* to valve control. Whereas *T-PM* has been applied to linear actuators [3.3] and to motors [3.4], this valve actuation application has not been considered previously.

Trans-Permanent Magnetics can be defined as the on-board process by which the polarity of permanent magnets is switched [3.5]. Note that the general principles employed in *T-PM* are similar to the general techniques used for off-board rapid magnetization [3.6]. The basic components in a trans-permanent magnetic system consist of a soft permanent magnet, a hard permanent magnet, a pulse coil, and a control circuit. In its simplest realization, a large current of short duration (pulse) flows through a pulse coil surrounding a soft magnet. The pulse changes the polarity of the soft magnet, thereby changing the state of the valve. As this chapter demonstrates, the needed control authority and the needed stroke in valve applications can be achieved using a linear stack of magnets. The potential reduction of power that is achievable with the trans-permanent valve results from the elimination of the power draw that otherwise exists to hold electromagnets in position during inactive periods. The potential reduction in actuation of power is extremely large in valves that operate infrequently. The potential decrease in mechanical wear that is achievable with the trans-

permanent magnetic valve results from the replacement of mechanical latching mechanisms with pulse-coils that have no moving parts. The potential decrease in electrical wear that is achievable with the *T-PM* valve results from the infrequent operation of the circuit. Like reduction of power, the potential reduction of wear, both mechanical and electrical, is extremely large in valves that operate infrequently.

The next section describes the principles of operation of *T-PM* valves. The relationships between the strength and number of permanent magnets in the linear stack and the stroke and resolution of the valve are developed in Section 3.3. Section 3.4 describes the alternating uniform linear stack and section 3.5 describes valve–spring design. The control circuit is developed in section 3.6. A prototype valve is introduced section 3.7 and is tested in section 3.8. Section 3.9 summarizes the results.

### **3.2 Principles of Operation**

Figure 3.1 depicts the basic components in a *T-PM* system [3.5]. As a general rule and as a matter of practical importance, the *B-H* magnetization curve is prohibitively steep, in the sense that it requires the application of prohibitively accurate electromagnetic fields to control the resulting level of magnetization [3.6]. Therefore, the purpose of on-board magnetization is only to change the polarity of the permanent magnet from one extreme to the other, that is, to switch the north and south poles of the magnet.

The change in polarity of a permanent magnet can be regarded as a binary operation. On the other hand, the number of desirable states of the valve may be more than two. In digital process valves, the states consist of the open state, the closed state, and possibly several intermediate states. In digital regulating valves, the digital states approximate a continuous function ranging between the open state and the closed state, so the number of states is relatively large. The constraints between stroke and resolution in a single pair of magnets allow for the design of a valve with only a few states. The ability to produce a larger number of valve states and the relaxation of the constraints between stroke and resolution are made possible by considering a linear stack of magnets instead of just a pair. Figure 3.2 depicts a linear stack of magnets. In general, the stack can consist of magnets of different field intensities and types - some hard and some soft. The question arises as to the relationship between the different ways the magnets are arranged and the resulting stroke and resolution. In the figure, identical hard magnets and identical soft magnets are alternated. In this arrangement, the hard magnets provide physical separation of the soft magnets from each other during polarization.

The control circuit is shown in Fig. 3.3. The control circuit consists of five functional blocks: Block 1 is the power input block. Block 2 preprocesses the signals before they're sent to blocks 3 and 4. Block 3 is a charge storage block. Block 4 is the processing block where logical operations are stored. Block 5 is the stack of permanent magnets and electromagnets. The circuit is described in detail in section 3.6.

### 3.3 Linear Stack Relationships

Consider a general linear stack of  $n$  magnets. Stiff cushions can be placed between the magnets. The cushions would be sufficiently stiff that their elastic deflections are negligibly small compared to the changes in the gaps between repelling magnets. Without loss of generality, assume that the right end of the stack is fixed and that the operation of the valve is governed by the position of a valve shaft, which is located to the left of the stack. The mathematical prediction of the precise magnetic force between any two repelling magnets can be a complex undertaking [3.4, 3.5]. The measurement of the magnetic force between any two repelling magnets is comparatively simple. Whether by prediction or by measurement, assume that the compressive magnetic force between the  $i$ -th magnet and the  $i+1$ -th magnet has been determined to be  $F = f_i(g)$ , where  $g$  denotes gap. A typical  $f_i(g)$  curve is shown in Fig. 3.4. The operating range of the gaps between the magnets is bound from below by a bearing friction force and bound from above by the strength of the magnets. The magnets across the stack are subjected to identical compressive forces that depend on the directions in which the magnets are polarized. The compressive force is magnetic between any two adjacent magnets that are polarized the opposite way and the compressive force is elastic between any two adjacent magnets that are polarized the same way. Let  $P = 1$  designate one direction a magnet is polarized and  $P = -1$  designate the opposite direction. Then the  $i$ -th gap is

$$g_i = \begin{cases} f_i^{-1}(F), & P_i = -P_{i+1} \\ 0, & P_i = P_{i+1} \end{cases}, (i = 1, 2, \dots, n-1) \quad (3.1)$$

where  $F$  is the compressive force. Assume that the orifice of the flow valve is positioned to the left of the stack along with a valve spring. Then  $F = k x$ , in which  $k$  denotes the valve spring constant and  $x$  denotes the compression of the spring. The valve–spring needs to always be in compression in order to keep the entire stack in compression and prevent slop. Indeed, the valve–spring is a key factor in the behavior of the valve; specifically, it determines the compressive force  $F$ .

A combination of gaps is associated with a particular way in which each of the magnets is polarized. Let the number of combinations of gaps be denoted by  $M$  (Note that  $M$  in Chapter 2 referred to magnetization). As shown in Fig. 3.5, the length  $L$  of the stack and the length  $D$  of the valve are

$$L^{(j)} = L_0 + \sum_{i=1}^{n-1} g_i^{(j)}, \quad D = L^{(j)} + l_0 - x^{(j)}, \quad (j = 1, 2, \dots, M) \quad (3.2a, b)$$

where  $L_0$  is the length of the magnets,  $g_i^{(j)}$  is the  $i$ -th gap associated with the  $j$ -th combination, and  $l_0$  is the unstretched length of the valve spring. The superscripts refer to the particular combinations of gaps. The range (stroke)  $R$  of the valve is defined as the difference between the length  $L^{(1)}$  of the stack when one gap is in magnetic repulsion and the length  $L^{(M)}$  of the stack when  $n - 1$  gaps are in magnetic repulsion, i.e., the first combination is associated with one gap in repulsion and the last combination is associated with all of the magnets in repulsion. From Eq. (3.2a)

$$R = L^{(M)} - L^{(1)} = \sum_{i=1}^{n-1} g_i^{(M)} - \sum_{i=1}^{n-1} g_i^{(1)}. \quad (3.3)$$

The force in the spring is

$$F^{(j)} = kx^{(j)}, (j = 1, 2, \dots, M) \quad (3.4)$$

Note that the spring force  $F^{(j)}$  is equal to the magnetic force between the magnets that are repelling each other. Letting  $j = 1$  and  $j = M$  in Eq. (3.4), we get from Eqs. (3.2) and (3.4)

$$R = x^{(M)} - x^{(1)}. \quad (3.5)$$

Note in general that  $x^{(M)} > x^{(1)}$  while  $g_i^{(M)} < g_i^{(1)}$ . Once hard and soft magnets are selected, Eqs. (3.4) through (3.6) can be used to specify the valve–spring as described later in the paper for the case of alternating uniform linear stacks.

The length  $L$  of the stack is called the state of the valve. In regulating valves, in which a continuous range of states is sought, the states can be ordered. The maximum difference between them yields the resolution  $E$  of the system. The performance parameters of the system are the range  $R$  and the resolution  $E$ . Determining the resolution of the system is clearly a combinatorial problem.

The primary design parameters in a trans-permanent valve, whether a process valve or a regulating valve, are the magnetic strengths of the magnets. They dictate the  $f_i(g)$  curves. The lengths of the magnets factor out of the range and resolution calculations, although they can enter into the design of the magnets, shielding, and the resulting fields.

Consider the six arrangements of hard and soft magnets shown in Fig. 3.6. In each arrangement, the left end is fixed and the right end is free. In the first arrangement, one soft magnet is employed. In the next two arrangements, two soft magnets are employed and in the last three arrangements three soft magnets are employed. The gap between two hard magnets has only one state, between two soft magnets has two states and between a soft and hard magnet has two states. It follows when hard and soft magnets are alternated that the number of soft magnets is minimized and the number of possible states is maximized. Also when soft and hard magnets are alternated the hard magnets shield the soft magnets from each other. Thus, it is generally recommended to alternate soft and hard magnets.

The interest lies in examining the number  $M$  of combinations of states  $L^{(j)}$ , ( $j = 1, 2, \dots, M$ ) that are achievable with a particular arrangement and the associated number  $N$  of independent design parameters. The number of independent design parameters is equal to the number of gaps  $n - 1$ . Indeed, the magnetic strengths of the soft and hard magnets can be selected to independently prescribe the gaps, at least in theory.

### 3.4 Alternating Uniform Linear Stacks

The following describes the cases that employ soft magnets of equal strength, and hard magnets of equal strength. These types of stacks are called uniform stacks. Although the stacks are uniform, the number of possible stack lengths can still be relatively large. With only one type of hard magnet and one type of soft magnet, there are still three magnetic force curves; they're associated with pairs of adjacent soft magnets, pairs of adjacent hard magnets, and pairs of adjacent hard and soft magnets. However, when the hard magnets and the soft magnets are alternated, there is only one magnetic force curve, reducing the number of possible gaps to two – the zero gap associated with equally polarized magnets and the non-zero gap associated with oppositely polarized magnets. The following considers alternating linear stacks (non-uniform) and then alternating uniform linear stacks.

First consider the number  $M$  of combinations of stack lengths in an alternating stack, which depends on the number  $n$  of magnets. In Fig. 3.6, the first, second, and forth arrangements were alternating, and the soft magnets were placed on the left ends of the stack. When the polarization of a soft magnet is changed, the lengths of two adjacent gaps surrounding the soft magnet change if the soft magnet is in the interior of the stack. If the soft magnet is on either end of the stack, then changing the polarization only affects the gap of the one magnet that is adjacent to it. It follows that the number of achievable states in alternating stacks is

$$M = 2^{\text{int}\left(\frac{n+1}{2}\right)}. \quad (3.6)$$

For the purposes of developing digital process valves employing alternating uniform stacks, the question arises as to the smallest number of magnets that yield  $M_D$  distinct states, where  $M_D$  is typically a small number (below 10), and as to the resolution that can be achieved. The number of distinct states in an alternating uniform stack is

$$M_D = n \quad (3.7)$$

From Eq. (3.6), the number of combinations of states in alternating stacks increases exponentially with the number of magnets. However, Eq. (3.7) shows that when the alternating stacks are uniform the number of distinct states increases linearly with the number of soft magnets. It follows as a general rule, that alternating uniform stacks are potentially well suited for digital process valves wherein the number of states is relatively small. On the other hand, non-uniform alternating stacks are potentially well suited for digital regulating valves (although the design process could be complicated), wherein the number of states is typically large.

### 3.5 Valve–Spring Design

As described earlier, the valve spring is a key factor in the behavior of the valve because it determines the compressive force  $F$  acting on each of the magnets. In the case of alternating uniform stacks, the valve–spring design becomes comparatively simple. The steps associated with determining the valve–spring are determined from Eqs. (3.3) through (3.5). They are summarized as follows:

Step 1: Select a pair of soft and hard magnets. This specifies the  $f(g)$  curve.

Step 2: Select  $F^{(1)}$  (corresponding to one magnet in repulsion) on the  $f(g)$  curve.  $F^{(M)}$  needs to be larger than the bearing friction force that is found in the system.

Step 3: Select the range  $R$  of operation and calculate the gap associated with  $F^{(M)}$  (i.e., when all of the magnets are in repulsion) from

$$g^{(M)} = \frac{R + g^{(1)}}{n-1}. \quad (3.8)$$

Step 4: Calculate  $F^{(M)}$  from the  $f(g)$  curve letting  $g = g_i^{(M)}$ .

Step 5: Calculate the valve–spring constant from

$$k = \frac{F^{(M)} - F^{(1)}}{R} \quad (3.9)$$

Step 6: Calculate the length of the valve  $D$  and the unstretched length  $l_0$  of the spring using the constraint

$$D - l_0 = L_0 + g^{(1)} - \frac{F^{(1)}}{k}. \quad (3.10)$$

### 3.6 Control Circuit

Figure 3.3 shows a photo and a schematic of the control circuit partitioned into 5 blocks, as mentioned earlier in the paper. The circuit specifications are given in Table 3.1.

In Block 1, diode  $U1$  and  $LED1$ , are placed ahead of the power switch and function as voltage protection for the control circuit. The switch in block 1 affects Blocks 2 and 3.

In Block 2, by closing the switch, current flows through the resistor  $R2$ , to reduce the 36 input voltage to the 12 volts needed for the LM7812 IC, which regulates the input voltage to the microprocessor in Block 4. Capacitors  $C1$  and  $C2$  are filters,  $C4$  and  $R5$  provide additional protection, and diode  $U3$  protects the microprocessor from possible back emf emanating from the inductors in Block 5.  $LED2$  indicates that Block 2 is properly charging the capacitor in Block 3.

In Block 3, by closing the switch in Block 1, current flows through resistor  $R4$  to charge up the capacitor bank  $C3$ . The Diode  $U2$  prevents  $C3$  from discharging into Block 1 and protects Block 1 from back *emf* emanating from Block 5. The value of  $C3$  and  $R6$  were selected to rapidly discharge the current in an over-damped manner [3.5].

Block 4 consists of two main parts – the BasicX-24 microcontroller (NetMedia, Inc. [3.7]) and the L298 high current dual full-bridge driver (STMicroelectronics, Inc. [3.8]). The microcontroller contains the instructions that operate the tunable magnets. It is externally

programmed in Basic by connecting to a host computer communication port (The corresponding code can be found in Appendix A). The L298 driver is responsible for switching the direction of the current flow through the tunable coils when the capacitor bank is being discharged. The driver can operate inductive loads up to 46V with continuous DC output currents up to 4A. The driver also contains over-temperature protection and high noise immunity. The microcontroller output commands the two L298 drivers to appropriately polarize the tunable coils. Although not shown in the schematic, ground resistors of 1 k $\Omega$  were used to ensure protection to the driver and two 10 k $\Omega$  resistors connected directly to the  $+V_{cc}$  input were used to protect the drivers from electric shock. The microcontroller easily provides enough source current to drive the internal L298 transistors into saturation. Detailed schematics of the microprocessor and the L298 are found in Appendix B.

Block 5 represents the permanent magnets and the tunable magnets (pairs of soft magnets and coils). The magnet types and sizes, and the number of turns in the coils were selected so that the current in the discharging capacitor was sufficiently high to enable the soft magnets to be fully polarized by the current in one direction or another (See Table 3.2).

### 3.7 Prototype Valve

The fourth arrangement given in Fig. 3.6 was prototyped. A photograph of the prototype valve is shown in Fig. 3.7. As shown, the prototype valve consists of  $n = 5$  magnets, three soft and two hard. The number of distinct states is  $M_D = n = 4$ . The two hard magnets in the system were set up so that their north poles were both on the left side of the system. This

way, the middle two gaps are either both in repulsion or both in attraction. The alternating uniform stack of three soft magnets and two hard magnets rides on linear bearings that slide along a central non-ferrous shaft. The linear bearings were press-fit into the centers of the annular shaped magnets. In the prototype, when the magnets are all in repulsion, the valve is fully closed, and when the magnets are all in attraction the valve is fully open. Stiff rubber dampers of 0.31 cm (0.122 in) in thickness were placed between each of the magnets. They serve the purposes of protecting the magnets from each other when making contact, and they decrease the force between any pair of attracting magnets, which later decreases the needed length of the valve spring.

The first step in the design process consisted of selecting the soft and hard magnets. The soft magnets are Alnico 5 and the hard magnets are Ceramic 8. The associated curve of the magnetic force versus the gap is shown in Fig. 3.4. Then the coils surrounding the soft magnets were designed (See Table 3.2). This part of the design process is described in detail in [3.5]. The remaining steps of the design process are particular to valves, and they were turned into the procedure described in Section 5 of this paper. Following this procedure, in step (1) a theoretical range of  $R = 1.2D_o = 0.538$  cm (0.212 in) was selected, in which  $D_o = 0.448$  cm (0.177 in) is the diameter of the valve orifice. In step (2), the spring force  $F^{(1)}$  was selected using the  $f(g)$  curve in Fig. 4.  $F^{(1)}$  needed to be larger than the maximum bearing friction force of 2.5 N (0.562 lb). As  $F^{(1)}$  is selected farther away from the friction limit, the spring constant becomes lower, which follows from Fig. 3.8, and Eqs. (3.8) and (3.9). For a robust design,  $F^{(1)}$  was selected in the “middle” of the curve at 17.25 N (3.88 lb) where  $g^{(1)} = 0.254$  cm (0.10 in). In step (3), the theoretical gap  $g^{(6)}$  of 0.134 cm (0.053 in) was calculated.

In step (4), the  $F^{(6)} = 17.92 \text{ N}$  (4.03 lb) was calculated. In step (5), the theoretical spring constant is  $k = 1.3 \text{ N/cm}$  (0.72 lb/in). In practice, 4 different springs were tested (More data using the other springs is provided in Appendix C); the spring constants of the tested springs are 1)  $k = 0.5 \text{ N/cm}$  (0.29 lb/in, 2)  $k = 0.6 \text{ N/cm}$  (0.34 lb/in, 3)  $k = 1.1 \text{ N/cm}$  (0.65 lb/in), and 4)  $k = 1.3 \text{ N/cm}$  (0.72 lb/in) (Century Springs, Inc. [3.10]). Using Eq. (3.11),  $D - l_0 = 1.56 \text{ in}$ . The following describes the testing of the prototype.

### 3.8 Testing

The testing of the system really began with the measurement of the magnetic force between the hard and soft magnets shown in Fig. 3.4. The magnetic force curve was generated as follows: The Alnico 5 magnet and the Ceramic 8 magnet were placed together in attraction with a spacer between. The thickness of the spacer is the gap  $g$ . Then, the magnets were hung; the Alnico 5 was placed on top and increasing amounts of weight were applied to the Ceramic 8 until it separated from the Alnico 5 magnet. This test was then repeated for different gaps. Note that the magnetization curve that was generated for attracting magnets is the same as the magnetization curve for repelling magnets. The measurement error was on the order of 9% [3.5].

The second test that was performed simply verified that the poles of the tunable magnets are successfully switched by the pulses. This test also verified the functionality of the control circuit.

The third test needed to measure the states  $L^{(j)}$ , ( $j = 1, 2, 3, 4$ ) of the valve. Although in theory there are  $M = 4$  states, in practice, there are more. For example, one gap in attraction while the others are in repulsion theoretically represents one state. The particular gap that is in attraction doesn't matter. In practice, however, there are 4 gaps, and the state depends on the particular gap that is in attraction because the magnets are not precisely uniform and because of errors caused by bearing friction. Therefore, instead of  $M_D = 4$  distinct states there are actually  $M = 2^{\text{int}\left(\frac{5+1}{2}\right)} = 8$  distinct states (using Eq. (3.6)). The combinations are numbered in Table 3.3, in which  $q$  denotes the number of magnets in repulsion.

The states were measured by setting up a linear variable differential transformer (LVDT) along the long axis on the valve directed toward the free end of the valve. The LDVT measurement was calibrated by setting to zero the displacement measurement when all of the magnets were in repulsion (the 8-th state). The measurement of the  $j$ -th state is therefore  $\Delta x^{(j)} = L^{(8)} - L^{(j)}$ , as shown in Table 3.4. Each test shown in Table 3.4 was run 4 times, verifying repeatability. Notice that  $\Delta x^{(2)} \cong \Delta x^{(3)}$ ,  $\Delta x^{(4)} \cong \Delta x^{(5)}$ , and  $\Delta x^{(6)} \cong \Delta x^{(7)}$ , as expected.

The second to last column of Table 3.4 gives the measurement estimates of the average gaps  $g_{av}^{(q)}$  between repelling magnets. The average gaps are calculated as follows: From Eqs. (3.2a,b) we obtain the linear equation of the spring force  $F^{(j)} = A + B^{(q)} g_{av}^{(q)}$ , where  $A = k(L_0 + l_0 - D)$  and  $B^{(q)} = kq$ . This linear equation is graphed in Fig. 3.8. The intersection of the spring force with the magnetic force curve yields the average gaps. The average gaps given in Table 3.4 are  $g_{av}^{(1)} = 0.254$  cm (0.1 in),  $g_{av}^{(2)} = 0.241$  cm (0.0948 in),

$g_{av}^{(3)} = 0.229 \text{ cm (0.09 in)}$ , and  $g_{av}^{(4)} = 0.216 \text{ cm (0.085 in)}$ . Notice that the average gaps decrease as more magnets are in repulsion, as expected. Overall, notice that the states are relatively well-spaced with respect to displacement. The displacement spacing between the  $q = 0$  and  $q = 1$  combination is  $0.114 \text{ cm (0.044 in)}$ , between the  $q = 1$  and  $q = 2$  combination is  $0.104 \text{ cm (0.041 in)}$ , between the  $q = 2$  and  $q = 3$  combination is  $0.083 \text{ cm (0.033 in)}$ , and between the  $q = 3$  and  $q = 4$  combination is  $0.142 \text{ cm (0.056 in)}$ . The displacement spacing represents the resolution  $E$  of the system.

The last test that was performed examined the flow rates through the air chamber to the right of the valve. The flow rates were measured using a digital anemometer (Power Instruments, Inc., Model 1717). In this test an input pressure of  $p_0 = 15 \text{ psi}$  was used on all of the tests shown in Table 3.5. As shown, similar to the displacement spacing, the flow rate spacing was relatively even. The flow rate spacing between the  $q = 0$  and  $q = 1$  combination is  $0.41 \text{ m/s (1.34 in/s)}$ , between the  $q = 1$  and  $q = 2$  combination is  $0.3 \text{ m/s (11.81 in/s)}$ , between the  $q = 2$  and  $q = 3$  combination is  $0.3 \text{ m/s (11.81 in/s)}$ , and between the  $q = 3$  and  $q = 4$  combination is  $0.3 \text{ m/s (11.81 in/s)}$ .

### 3.9 Summary and Conclusions

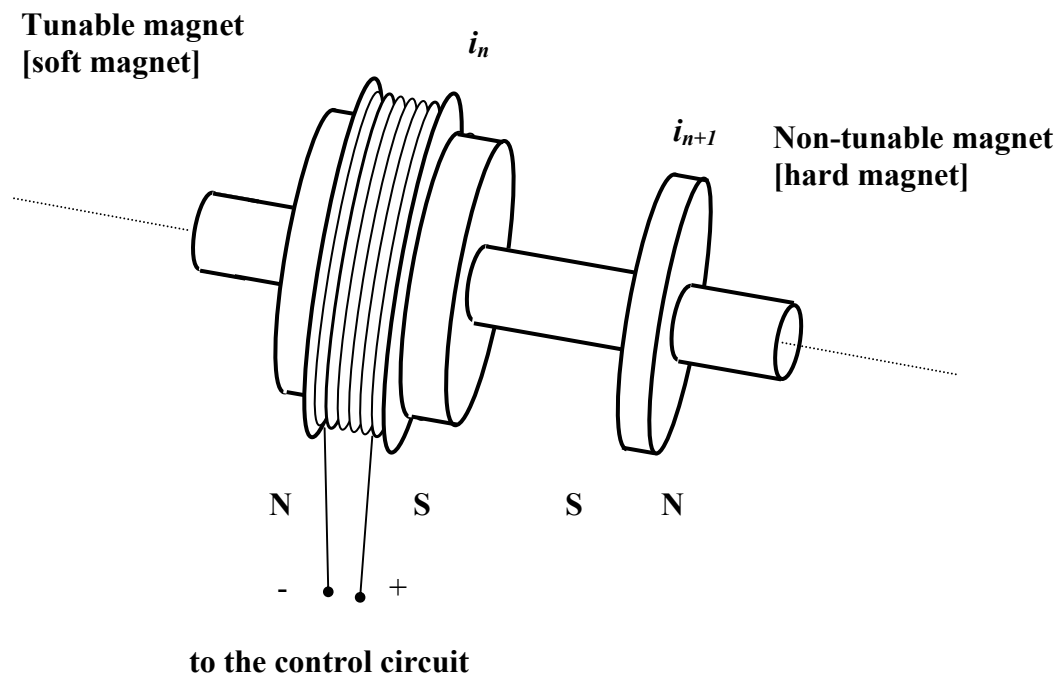
The principles of operation of a trans-permanent magnetic valve were first described – including the basic components that make up a trans-permanent magnetic system and the general arrangement associated with a stack of magnets. Next, the relationships between the magnetic forces, the spring forces, and the states in a stack of magnets were developed.

General stacks were first considered followed by uniform alternating stacks. It was shown that the uniform stack is well-suited to digital process valves in which the number of states is typically small and not very well-suited to digital regulating valves. Then a 6-step procedure was developed for the design of the valve-spring, thereby completing the paper's theoretical developments. Next, a laboratory prototype of a uniform alternating stack was designed and fabricated. It was comprised of five magnets – three soft and two hard, which theoretically had eight distinct states. The testing of the prototype was then presented. The testing results verified the performance of trans-permanent valves. The laboratory prototype valve was capable of controlling flow rates between 0 and 1.58 m/s (62.2 in/s) with a resolution of 0.3 m/s (11.81 in/s) with only 15 psi. The valve states ranged between 0 and 0.504 cm (0.198 in) with a resolution of 0.114 cm (0.044 in). In general, the laboratory prototype successfully verified the feasibility of the technology. Its cost-effectiveness would need to be verified in the development of a prototype tailored to a particular product class.

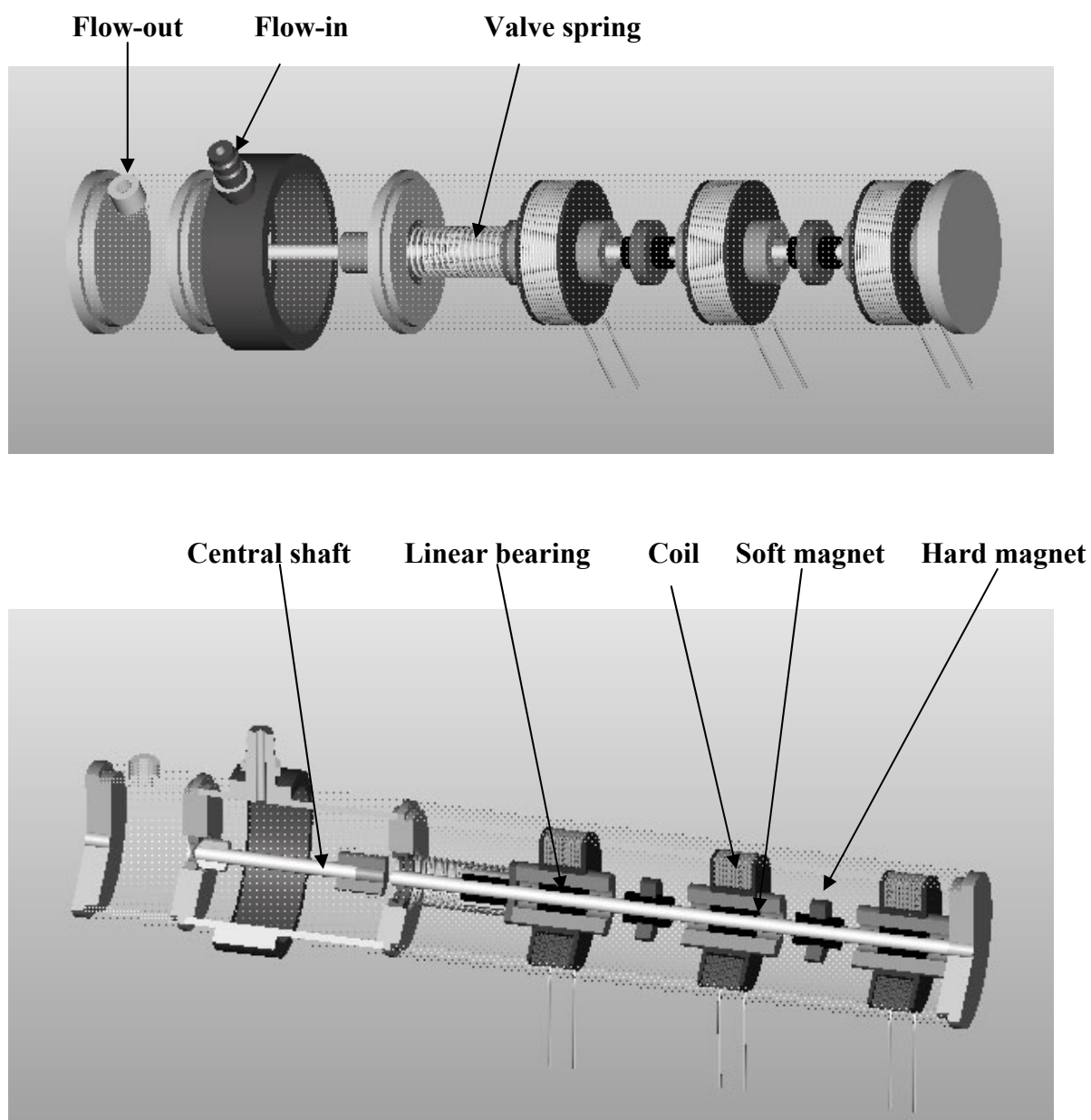
### 3.10 References

- 3.1 Sethson, K. M. R. (1993), "Identifying the Dynamics of Fast Response Solenoid Valves," The Third International Conference on Fluid Power, Linkoping 25-26, May 1993, pp. 271-287.
  
- 3.2 Becker, U. and Schnieder, E. (1993) "Different Mode of Operation of Pulse-Modulation with the Drive of 2/2 Fast Switching Valves," The Third Scandinavian International Conference of Fluid Power, May 1993, Sweden, pp. 237-254.
  
- 3.3 Silverberg, L. and Farmer, D. (2003) "On Trans-Permanent Magnetic Actuation for Spacecraft Pointing, Shape Control, and Deployment," Journal of Spacecraft and Rockets, to appear.
  
- 3.4 Farmer, D. (2003) "Trans-Permanent Actuators and Motors," Ph.D. Dissertation, Mechanical Engineering, North Carolina State University, Raleigh, NC, 27695-7910.
  
- 3.5 Silverberg, L. and L. Duval, 2003, "Analysis of Trans-Permanent Magnetic Systems", Journal of Dynamic Systems, Measurement and Control, 125(1), pp. 143-146.
  
- 3.6 Zycki, Z. and Pawluk, K. (1998) "Design of RLC Circuit for Pulse Magnetizer of Permanent Magnets," Int. J. for Computation and Mathematics in Electrical and Electronic Engineering, 17(1, 2, 3), pp. 412-417.

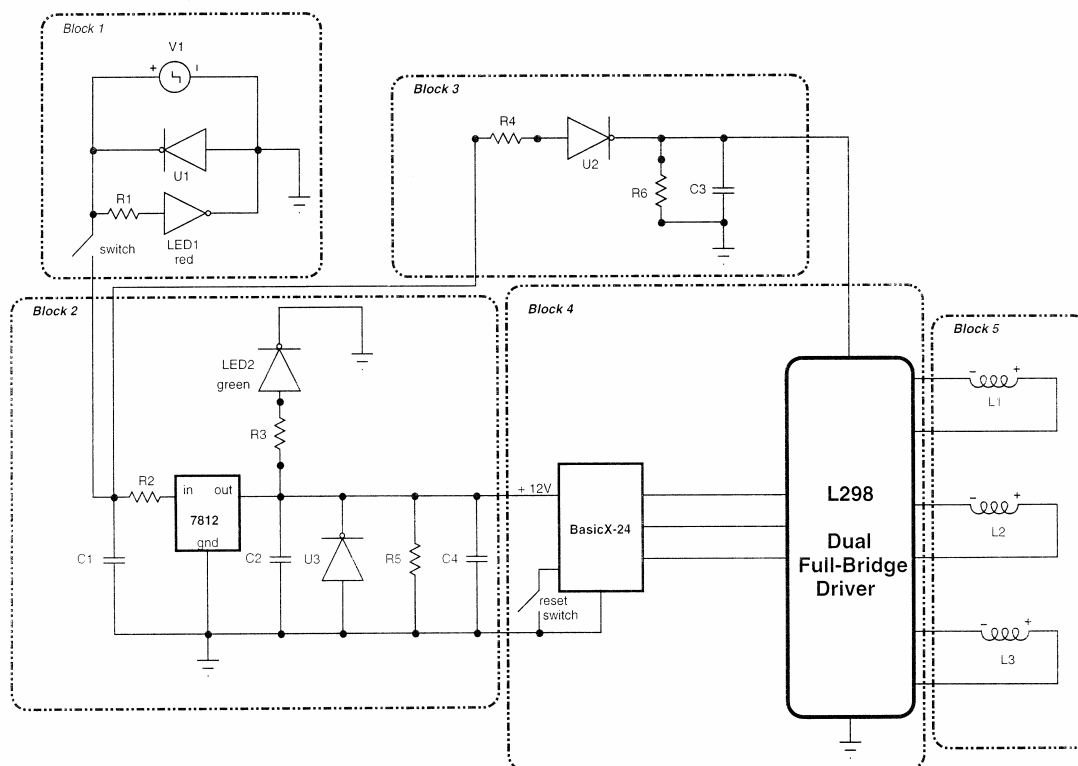
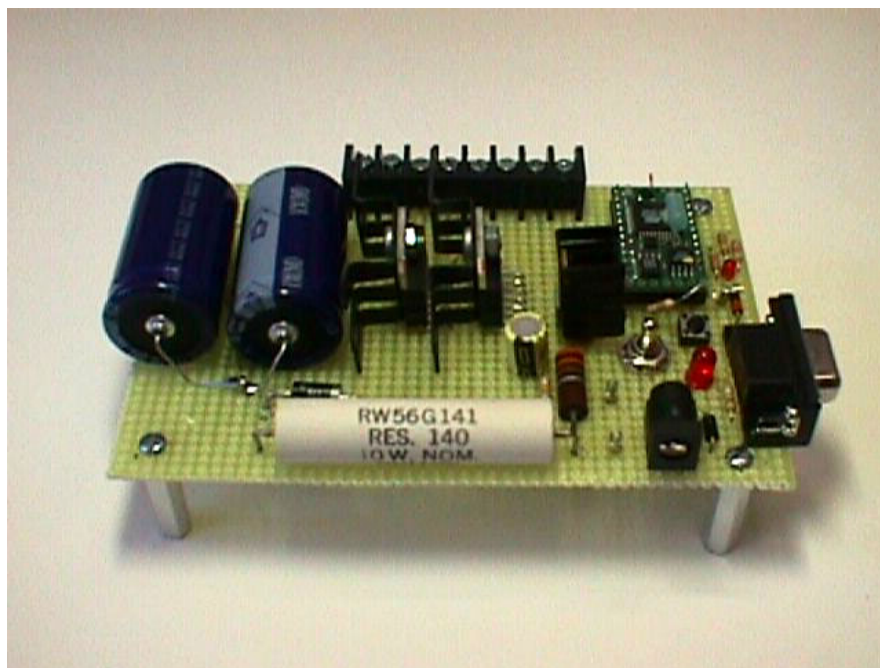
- 3.7 BasicX-24 Microcontroller. NetMedia Inc. ([www.basicx.com](http://www.basicx.com))
- 3.8 L298 Dual Full-Bridge Driver Datasheet. STMicroelectronics ([www.st.com](http://www.st.com))
- 3.9 Duval, L. (2003), “Low Power Valve Actuation using Trans-Permanent Magnetics,”  
Ph.D.Dissertation, Mechanical Engineering, North Carolina State University,  
Raleigh, NC 27695-7910.
- 3.10 Spring Catalog 2002. Century Spring Corp. ([www.centuryspring.com](http://www.centuryspring.com))



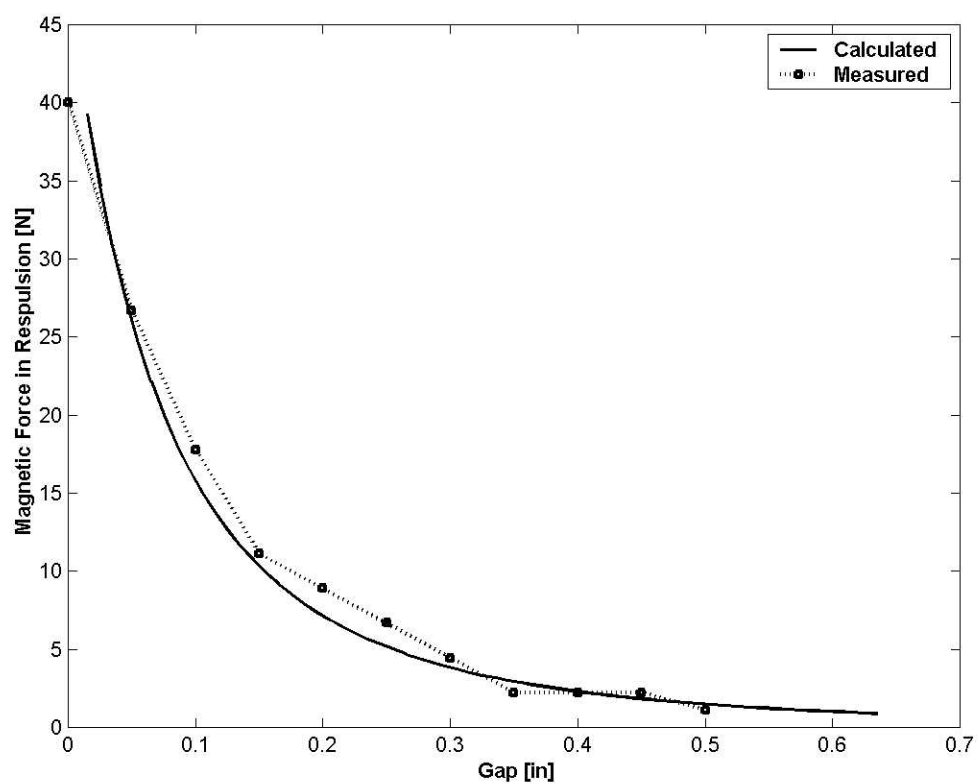
**Figure 3.1** *T-PM* System



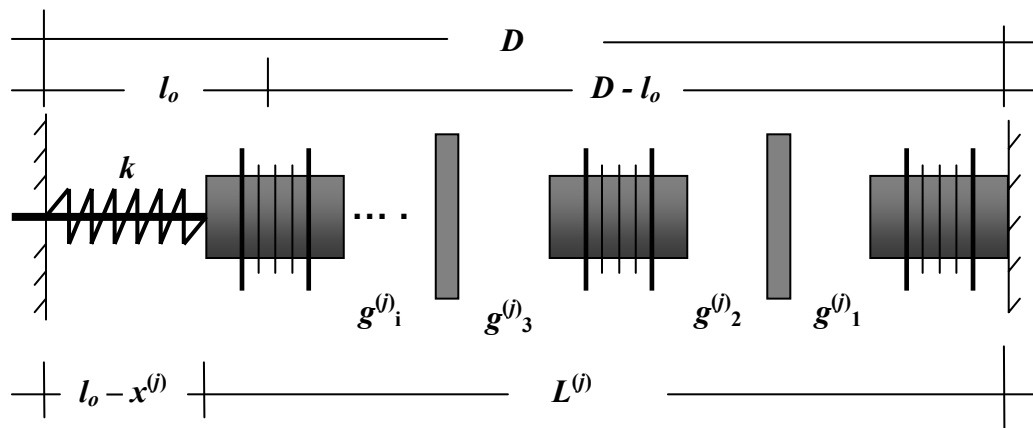
**Figure 3.2 Linear Stack of Magnets (complete view and cut away)**



**Figure 3.3 Photo and Schematic of the Control Circuit**
























**Figure 3.4 Measured Force versus Gap Curve (Alnico 5 and Ceramic 8)**



$L_o$  = Length of  $n$ -magnets  
 $l_o$  = unstretched length of valve spring

Figure 3.5 Stack Geometry

		1	2	3	4	$M$	$M_D$
1	{					2	2
2	{					4	3
						4	4
3	{					8	4
						8	1
						8	8


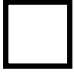
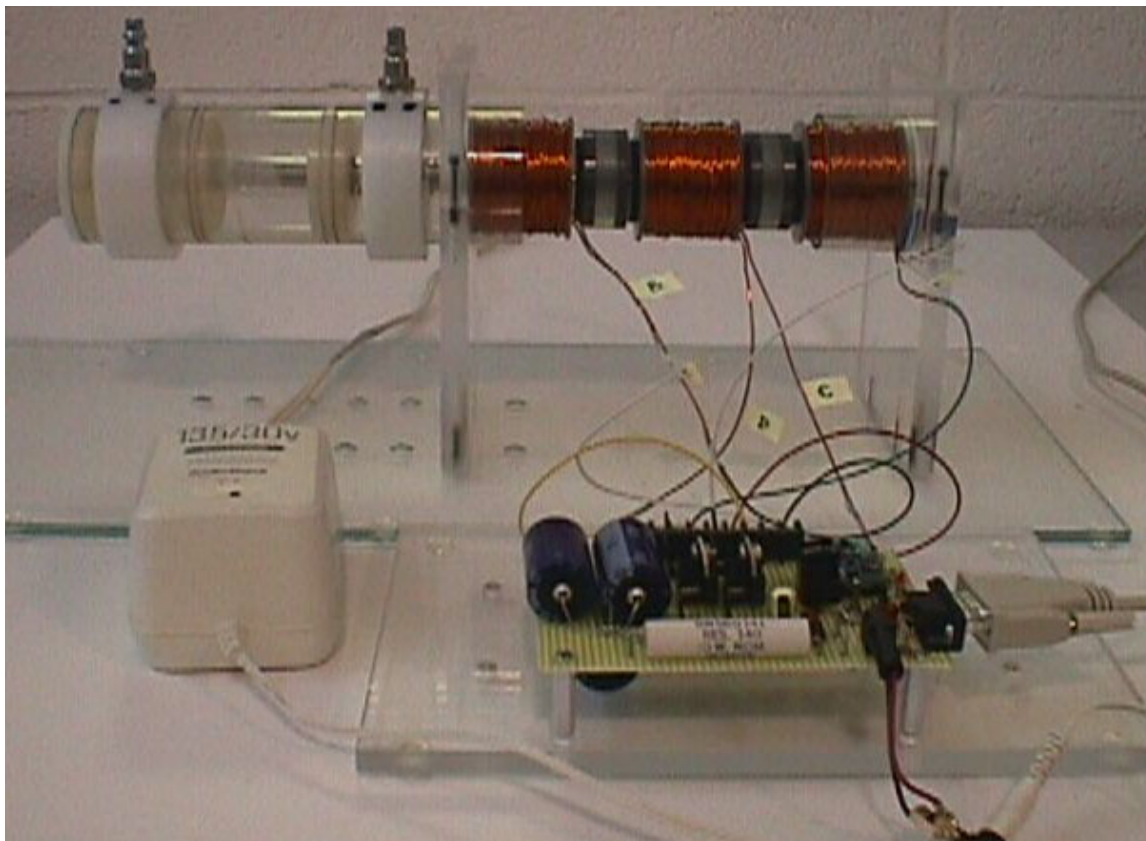
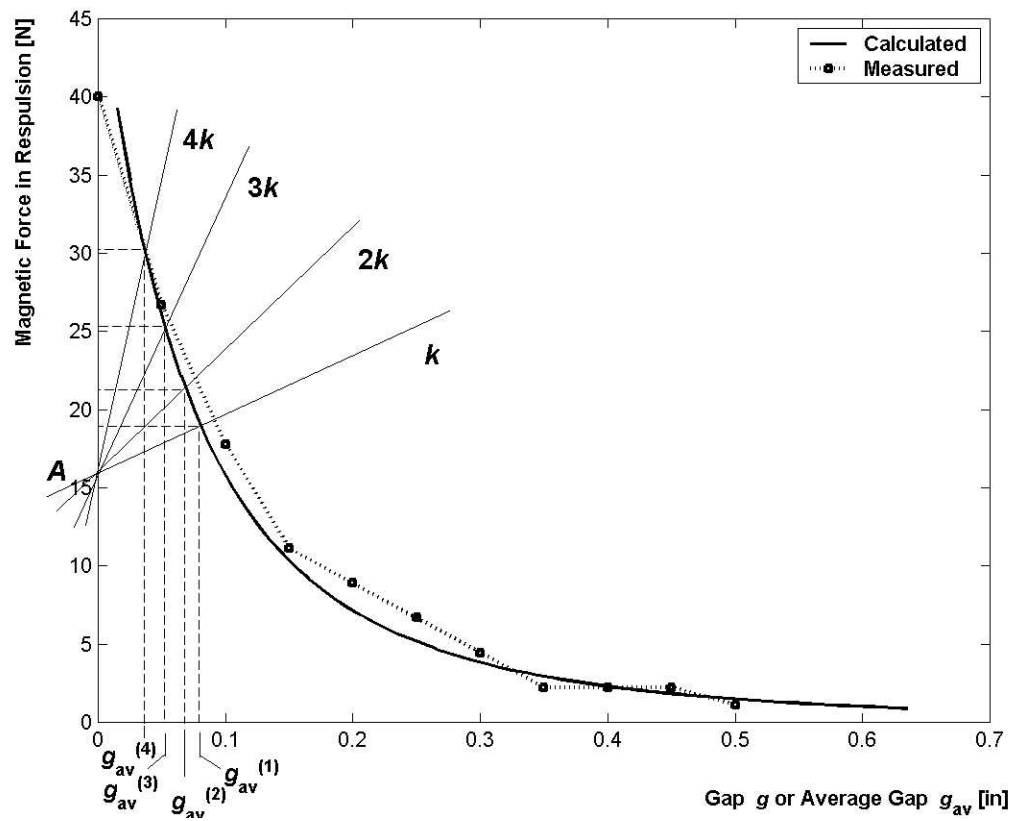
 = Tunable magnet  
 = Non-tunable

Figure 3.6 Magnet Arrangements



**Figure 3.7** Prototype Valve



**Figure 3.8 Design Curve for Valve Spring**  
 ( $k = 1.3 \text{ N/cm}$ ,  $A = 16.94 \text{ N}$ )

Table 3.1 Circuit Specifications

Name	Values
<i>Resistors</i>	
R1	3.6 k $\Omega$
R2	620 $\Omega$ , 1W
R3	1 k $\Omega$
R4	120 $\Omega$ , 15W
R5, R6	10 k $\Omega$
<i>Diodes</i>	
U1, U2, U3, U4, U5, U6	IN4007
<i>Capacitors</i>	
C1, C2	100 $\mu$ F
C3	3 units 4700 $\mu$ F, 35V (Capacitor Bank) 0.0141 F
C4	0.22 $\mu$ F
<i>LED</i>	
LED1, LED2	LiteOn™ $V_f = 1.2$ , $V_r = 5$ $I$ (mA) = 50
<i>Voltage Regulator</i>	
	7812 IC
<i>Dual Full-Bridge Driver :</i>	L298 STMicroelectronics™
<i>Micro-Controller</i>	
BasicX-24 NetMedia, Inc.™	16 total I/O lines (8 TTL plus 8 ADCs and or TTL) 1200 to 19200 Baud buffered serial 400 bytes of RAM IEEE floating point math
<i>Power Supply</i>	
V1	13.5-30 V-DC/1000 mA AC-to-DC Adapter Switching Type Radio Shack™

Table 3.2 Magnetic Material and Coil Design

Magnets	<u>Alnico 5:</u>  Outer Diameter $R_2$ , in Inner Diameter $R_1$ , in Length $l_1$ , in  <u>Ceramic 8:</u>  Outer Diameter $R_2$ , in Inner Diameter $R_1$ , in Length $l_2$ , in	1.25 0.31 1.75  1.50 0.80 0.20
Coil	Number of turns $N$ Type of Wire Inductance $L$ , H Resistance $R$ , $\Omega$	350 18 AWG $2.5 \times 10^3$ 0.9

**Table 3.3 Numbering of Gap Combinations**

$j$	$q$	$g_1$	$g_2$	$g_3$	$g_4$
1	0	-	-	-	-
2	1	+	-	-	-
3		-	-	-	+
4	2	-	+	+	-
5		+	-	-	+
6	3	+	+	+	-
7		-	+	+	+
8	4	+	+	+	+

**+ = Repulsion**

**- = Attraction**

Table 3.4 Test Results ( $k = 1.3$  N/cm)

$j$	$q$	$g_1$	$g_2$	$g_3$	$g_4$	$\Delta x_{av}^*$	$\sigma_{\Delta x_{av}}^*$	$g_{av}^*$	$\sigma_{g_{av}}^*$
1	0	-	-	-	-	0.0	---	---	---
2	1	+	-	-	-	0.114	0.0041	0.254	0.0095
3		-	-	-	+	0.124	0.0042		
4	2	-	+	+	-	0.228	0.0404	0.241	0.0144
5		+	-	-	+	0.253	0.0340		
6	3	+	+	+	-	0.336	0.0235	0.229	0.0087
7		-	+	+	+	0.362	0.0333		
8	4	+	+	+	+	0.504	0.0219	0.216	0.0047

\* Average generated by repeating test 4 times.

**Table 3.5 Test Results ( $k = 1.3$  N/cm,  $p_0 = 15$  psi )**

$j$	$q$	$V_{av}^*$	$\sigma_{V_{av}}^*$
1	0	1.5837	0.0523
2/3	1	1.1722	0.0224
4/5	2	0.8801	0.0256
6/7	3	0.5867	0.0225
8	4	0.2603	0.0127

\* Average generated by repeating test 4 times.

## **Chapter 4**

### **Recommendations**

## 4.1 Recommendations and Conclusions

The work contained in this dissertation represents a beginning look at *T-PM*. To fully realize the capabilities developed in this dissertation, the laboratory prototypes that were developed will need to be extended to manufacturing prototypes. The manufacturing prototypes will need to be tested. Appropriate markets will need to be identified. Field tests would need to be performed. And that is only the beginning.

The following recommendations and conclusions pertain to *T-PMs* in general, and more specifically to *T-PM* valves.

### 4.1.1 General Recommendations

When a manufacturing prototype is being developed it is recommended that several important issues be given special attention. The following four issues have been identified as the most important:

- Packaging
- Rapid Switching
- Optimal Coil Design
- Scaling

Package compactness is an important issue that depends largely on the particular application. However, there are several issues about packaging that can be looked at early on, independent of the application. In particular, the configuration of the circuit, the use of

smaller components in the circuit, the use of two-sided boards, and heat rejection limitations need to be examined.

The rate at which the magnets can be switched has not been minimized. While this may not be important in many applications, rapid switching can open up possibilities in other applications. Moreover, there may be reasons that are ancillary for developing rapid switching. For example, by studying rapid switching a better understanding of how to minimize the field currents, and reduce wear could be reached.

Through optimal coil design, the nominal geometry of the magnets can be modified and parametric design studies, which are commonly used in controlled experiments, can be conducted to study the interactive effect of various parameters on a particular response or responses.

The prototype valve is about twice the size of comparable industry valves. However, through optimization, it is anticipated that the scale of the system could be reduced by a factor of 3 or 4. To reduce the scale, the geometry of the magnet would need to be examined closely. The number of coils can be reduced. The interference between the magnets can be minimized to reduce the long dimension of the system. The tolerances can be improved to create a tighter and smaller system.

#### **4.1.2 Conclusions and Recommendations Pertaining to Valves**

The following general conclusions about *T-PM* valves have been compiled:

1. The *T-PM* method was successfully applied to a valve and demonstrated in a laboratory prototype.
2. A procedure was developed for the design of the valve spring. The procedure is applicable to any number of magnets in the stack.
3. General relationships (applicable to any number of magnets in the stack) were developed relating to resolution, the number of states, and design complexity. It was concluded that uniform alternating stacks of magnets leads to a relatively simple and orderly design procedure, but that non-uniform alternating stacks, which would be required in order to achieve a reasonable number of states in regulating valves, leads to a rather complex design procedure, from which it appears that T-PM stacks are not well-suited for regulating valves.
4. The work done by a linear stack increases proportionally with the number of gaps. Therefore, the number of magnets can be selected to satisfy the work requirements of the valve (even when the interest lies in using the T-PM only as an on-off valve).
5. In the case of a non-uniform linear stack, the T-PM valve can be used as a “check valve” (which is used to set the flow pressure).
6. An elegant and compact analog circuit was developed that was composed of only 3 primary part types (2 drivers, 1 processor, 3 capacitors).

7. By charging the capacitors just before they are to be discharged, the power requirements of the T-PM valve become proportional to the number of times the valve is switched on a per unit of time basis, reducing the power requirement of the T-PM valve to be orders of magnitude lower than for a conventional valve, depending on the usage of the valve.

Future recommendations pertaining to valves are:

- Identify product application and develop manufacturing prototype
  - o Possibly focus on a small number of permanent magnets to bring out the fundamental advantages of *T-PMs*.
- Conduct reliability test.
- Optimize design to meet specific requirements:
  - o Reduce bearing friction
  - o Topology (take advantage of electromechanical force)
  - o Reduce size (Scale)

### 4.1.3 Unanswered Questions

Although there are certainly many unanswered questions with *T-PM*, the following ones appear to me to be particularly important.

- 1) The complexity of the *T-PM* circuit is more complex than in a traditional valve. This is a distinct disadvantage that. It is unclear to what extent this complexity is a problem.
- 2) The holding force using *T-PM* is accomplished using permanent magnets in contrast with the solenoid. The solenoid performs the holding force using electromagnets. This means, that the holding force using *T-PM* is generally weaker than using other used methods. It is not clear to what extent this limits the applicability of the method.
- 3) As a method that is in its early stage of development and that has not been “assigned” a product, it is unclear whether better performance can be achieved at a reduced manufacture cost

## **Appendix A**

### **BasicX-24 Code**

```

Dim t As Single 'Set variable t as a Single
Dim q As Single 'Set variable q as a Single
Dim s As Single 'Set variable s as a Single

Sub Main()

t = 0.002 'Time for pulse (Discharging time)
q = 30.0 'Time delay between pulses to read LVDT output
s = 10.0 'Time for reset all magnets in repulsion

Do

'Scenario 1
Call Reset
Call Delay(q)

'Scenario 2
Call Putpin(11,0) 'Set initial polarity X and Y - attraction
Call Putpin(12,1)

Call PulseOut(10,t,1) 'Pulse Solenoid 1
Debug.Print "pulse on 10"
Call Delay(q)

Call Reset()

'Scenario 5
Call Putpin(11,0) 'Set initial polarity X and Y - attraction
Call Putpin(12,1)

Call PulseOut(8,t,1) 'Pulse Solenoid 3
Debug.Print "pulse on 8"
Call Delay(q)

Call Reset()

'Scenario 8
Call Putpin(11,0) 'Set initial polarity X and Y - attraction
Call Putpin(12,1)

Call PulseOut(10,t,1) 'Pulse Solenoid 1
Debug.Print "pulse on coil #10"
Call PulseOut(8,t,1) 'Pulse Solenoid 3
Debug.Print "pulse on 8"
Call Delay(q)

Call Reset()

'Scenario 9
Call Putpin(11,0) 'Set initial polarity X and Y - attraction
Call Putpin(12,1)

Call PulseOut(9,t,1) 'Pulse Solenoid 2
Debug.Print "pulse on 9"
Call Delay(q)

Call Reset()

```

```

'Scenario 16
Call Putpin(11,0) 'Set initial polarity X and Y - attraction
Call Putpin(12,1)

Call PulseOut(10,t,1)      'Pulse Solenoid 1
Debug.Print               "pulse on 10"
Call PulseOut(9,t,1)      'Pulse Solenoid 2
Debug.Print               "pulse on 9"
Call PulseOut(8,t,1)      'Pulse Solenoid 3
Debug.Print               "pulse on 8"
Call Delay(q)

Call Reset()

Loop

End Sub

Sub Reset()               'Set all tunable magnets in repulsion

Call Putpin(11,1) 'Reverse Polarity of X and Y
Call Putpin(12,0)

Call PulseOut(8,t,1)      'Pulse Solenoid 3
Debug.Print               "pulse on 8"

Call PulseOut(9,t,1)      'Pulse Solenoid 2
Debug.Print               "pulse on 9"

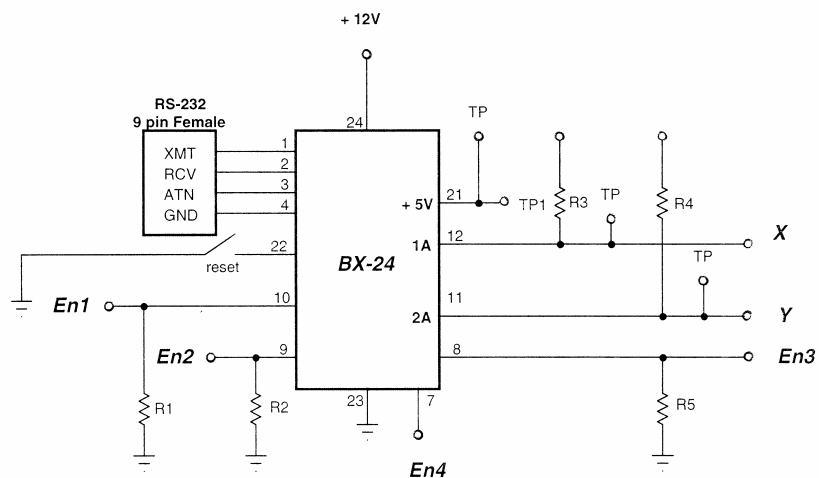
Call PulseOut(10,t,1)     'Pulse Solenoid 1
Debug.Print               "pulse on 10"
Call Delay(s)

End Sub

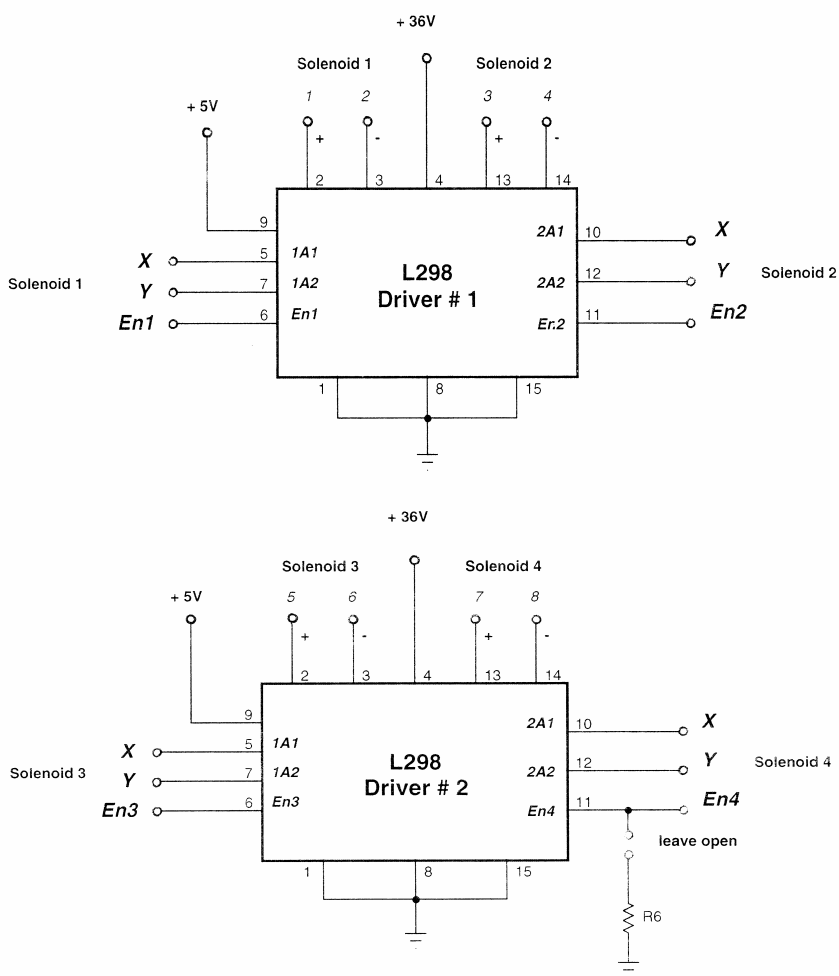
```

## **Appendix B**

### **BasicX-24 and L298 Connections**



## BasicX-24 Connections



## **Appendix C**

### **Springs Test**

**Case 1: Spring 12696 [Rate = 0.72 lb/in]****Test 1**

<i>j</i>	g1	g2	g3	g4	in	cm
1	0	0	0	0	0	0
2	1	0	0	0	0.0457	0.116078
3	0	0	0	1	0.0482	0.122428
4	0	1	1	0	0.095	0.2413
5	1	0	0	1	0.11	0.2794
6	1	1	1	0	0.13	0.3302
7	0	1	1	1	0.14	0.3556
8	1	1	1	1	0.1986	0.504444

**Test 2**

<i>j</i>	g1	g2	g3	g4	in	cm
1	0	0	0	0	0	0
2	1	0	0	0	0.046	0.11684
3	0	0	0	1	0.051	0.12954
4	0	1	1	0	0.0865	0.21971
5	1	0	0	1	0.0893	0.226822
6	1	1	1	0	0.125	0.3175
7	0	1	1	1	0.13	0.3302
8	1	1	1	1	0.1818	0.461772

**Test 3**

<i>j</i>	g1	g2	g3	g4	in	cm
1	0	0	0	0	0	0
2	1	0	0	0	0.0452	0.114808
3	0	0	0	1	0.047	0.11938
4	0	1	1	0	0.108	0.27432
5	1	0	0	1	0.1125	0.28575
6	1	1	1	0	0.146	0.37084
7	0	1	1	1	0.161	0.40894
8	1	1	1	1	0.201	0.51054

**Test 4**

<i>j</i>	g1	g2	g3	g4	in	cm
1	0	0	0	0	0	0
2	1	0	0	0	0.0425	0.10795
3	0	0	0	1	0.0489	0.124206
4	0	1	1	0	0.07	0.1778
5	1	0	0	1	0.087	0.22098
6	1	1	1	0	0.129	0.32766
7	0	1	1	1	0.1392	0.353568
8	1	1	1	1	0.196	0.49784

**Case 2: Spring 3340 [Rate = 0.65 lb/in]****Test 1**

<i>j</i>	g1	g2	g3	g4	in	cm
1	0	0	0	0	0	0
2	1	0	0	0	0.0532	0.135128
3	0	0	0	1	0.059	0.14986
4	0	1	1	0	0.108	0.27432
5	1	0	0	1	0.119	0.30226
6	1	1	1	0	0.175	0.4445
7	0	1	1	1	0.1801	0.457454
8	1	1	1	1	0.248	0.62992

**Test 2**

<i>j</i>	g1	g2	g3	g4	in	cm
1	0	0	0	0	0	0
2	1	0	0	0	0.055	0.1397
3	0	0	0	1	0.059	0.14986
4	0	1	1	0	0.118	0.29972
5	1	0	0	1	0.121	0.30734
6	1	1	1	0	0.178	0.45212
7	0	1	1	1	0.185	0.4699
8	1	1	1	1	0.251	0.63754

**Test 3**

<i>j</i>	g1	g2	g3	g4	in	cm
1	0	0	0	0	0	0
2	1	0	0	0	0.0524	0.133096
3	0	0	0	1	0.056	0.14224
4	0	1	1	0	0.108	0.27432
5	1	0	0	1	0.1125	0.28575
6	1	1	1	0	0.169	0.42926
7	0	1	1	1	0.17	0.4318
8	1	1	1	1	0.232	0.58928

**Test 4**

<i>j</i>	g1	g2	g3	g4	in	cm
1	0	0	0	0	0	0
2	1	0	0	0	0.054	0.13716
3	0	0	0	1	0.058	0.14732
4	0	1	1	0	0.108	0.27432
5	1	0	0	1	0.113	0.28702
6	1	1	1	0	0.167	0.42418
7	0	1	1	1	0.176	0.44704
8	1	1	1	1	0.24	0.6096

**Case 3: Spring GG-43 [Rate = 0.34 lb/in]****Test 1**

<i>j</i>	g1	g2	g3	g4	in	cm
1	0	0	0	0	0	0
2	1	0	0	0	0.078	0.19812
3	0	0	0	1	0.089	0.22606
4	0	1	1	0	0.172	0.43688
5	1	0	0	1	0.179	0.45466
6	1	1	1	0	0.257	0.65278
7	0	1	1	1	0.268	0.68072
8	1	1	1	1	0.365	0.9271

**Test 2**

<i>j</i>	g1	g2	g3	g4	in	cm
1	0	0	0	0	0	0
2	1	0	0	0	0.08	0.2032
3	0	0	0	1	0.093	0.23622
4	0	1	1	0	0.1801	0.457454
5	1	0	0	1	0.187	0.47498
6	1	1	1	0	0.261	0.66294
7	0	1	1	1	0.28	0.7112
8	1	1	1	1	0.38	0.9652

**Test 3**

<i>j</i>	g1	g2	g3	g4	in	cm
1	0	0	0	0	0	0
2	1	0	0	0	0.08	0.2032
3	0	0	0	1	0.086	0.21844
4	0	1	1	0	0.168	0.42672
5	1	0	0	1	0.17	0.4318
6	1	1	1	0	0.243	0.61722
7	0	1	1	1	0.26	0.6604
8	1	1	1	1	0.35	0.889

**Test 4**

<i>j</i>	g1	g2	g3	g4	in	cm
1	0	0	0	0	0	0
2	1	0	0	0	0.075	0.1905
3	0	0	0	1	0.084	0.21336
4	0	1	1	0	0.17	0.4318
5	1	0	0	1	0.165	0.4191
6	1	1	1	0	0.258	0.65532
7	0	1	1	1	0.264	0.67056
8	1	1	1	1	0.35	0.889

**Case 4: Spring S-490 [Rate = 0.29 lb/in]****Test 1**

<i>j</i>	g1	g2	g3	g4	in	cm
1	0	0	0	0	0	0
2	1	0	0	0	0.091	0.23114
3	0	0	0	1	0.1	0.254
4	0	1	1	0	0.194	0.49276
5	1	0	0	1	0.2	0.508
6	1	1	1	0	0.28	0.7112
7	0	1	1	1	0.3	0.762
8	1	1	1	1	0.42	1.0668

**Test 2**

<i>j</i>	g1	g2	g3	g4	in	cm
1	0	0	0	0	0	0
2	1	0	0	0	0.096	0.24384
3	0	0	0	1	0.1	0.254
4	0	1	1	0	0.198	0.50292
5	1	0	0	1	0.216	0.54864
6	1	1	1	0	0.3	0.762
7	0	1	1	1	0.321	0.81534
8	1	1	1	1	0.45	1.143

**Test 3**

<i>j</i>	g1	g2	g3	g4	in	cm
1	0	0	0	0	0	0
2	1	0	0	0	0.07	0.1778
3	0	0	0	1	0.09	0.2286
4	0	1	1	0	0.176	0.44704
5	1	0	0	1	0.198	0.50292
6	1	1	1	0	0.261	0.66294
7	0	1	1	1	0.293	0.74422
8	1	1	1	1	0.4	1.016

**Test 4**

<i>j</i>	g1	g2	g3	g4	in	cm
1	0	0	0	0	0	0
2	1	0	0	0	0.0904	0.229616
3	0	0	0	1	0.99	2.5146
4	0	1	1	0	0.2002	0.508508
5	1	0	0	1	0.209	0.53086
6	1	1	1	0	0.3	0.762
7	0	1	1	1	0.315	0.8001
8	1	1	1	1	0.43	1.0922